

**Efficient Access to A Designer Phosphapalladacycle Catalyst
via Enantioselective Catalytic Asymmetric Hydrophosphination**

Xi-Rui Li, Xiang-Yuan Yang, Yongxin Li, Sumod A. Pullarkat, Pak-Hing Leung*

[^a] Division of Chemistry & Biological Chemistry, School of Physical and Mathematical Sciences, Nanyang Technological University, Singapore 637371, Singapore Fax: (+65) 6791 1961; e-mail: pakhing@ntu.edu.sg.

Supporting Information

Table of Contents	S1
General Information	S2
Experimental Section	S2-7
Reference	S7
NMR Spectra	S8-20
HPLC Spectra	S21-29
Selected Bond Lengths (Å) of Complexes 12b, 13, 15 and 20	S30
Crystallographic Data	S31-46

General Information

All reactions were carried out under a positive pressure of nitrogen using standard Schlenk technique. NMR spectra were recorded on Bruker AV 300, AV500 and BBFO 400 spectrometers. Chemical shifts were reported in ppm and referenced to an internal SiMe₄ standard (0 ppm) for ¹H NMR, chloroform-d (77.00 ppm) for ¹³C NMR, and an external 85% H₃PO₄ for ³¹P{¹H} NMR. Acetonitrile (MeCN), dichloromethane (DCM), chloroform, *n*-hexane, acetone, ethyl acetate (EA) and methanol (MeOH) were purchased from their respective companies and used as supplied. Tetrahydrofuran (THF) was distilled from sodium/benzophenone prior to use. Solvents were degassed when necessary. A Low Temp Pairstirrer PSL-1800 was used for controlling low temperature reactions. Column chromatography was carried out with Silica gel 60 (Merck). Melting points were measured using SRS Optimelt Automated Point System SRS MPA100. Optical rotation were measured with JASCO P-1030 Polarimeter in the specified solvent in a 0.1 dm cell at 22.0°C. The enantioselectivities of the hydrophosphination reactions were determined with Agilent 1200 Series High Performance Liquid Chromatography (HPLC) machine fitted with a Daicel Chiralpak IC column and eluted with a mixture of *n*-hexane/2-propanol at 23°C.

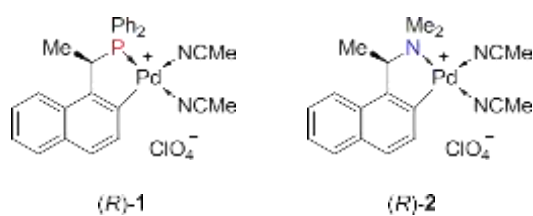
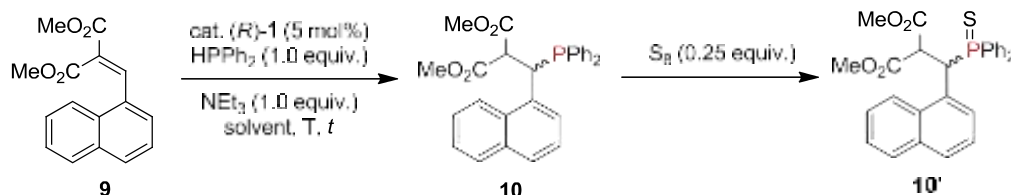


Figure s1. Molecular structures of PC-catalyst **1** and NC-catalyst **2**.

Caution! Perchlorate salts of metal complexes are potentially explosive compounds and should be handled with care.

The PC-catalyst **1**,¹ NC-catalyst **2**,² benzylamine palladium complex **11**³ and unsaturated malonate **9**⁴ were prepared according to literature methods. All other reactants and reagents were used as supplied without further purification unless stated otherwise.

General procedure for asymmetric hydrophosphination with PC-catalyst (R)-1.

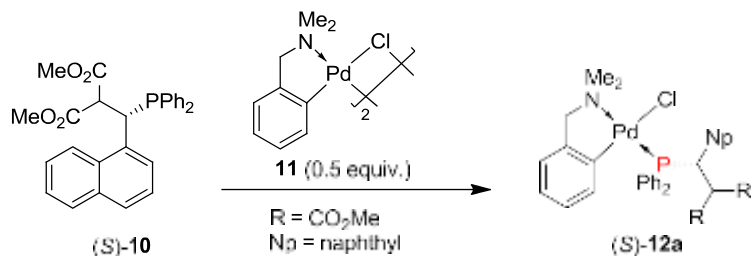


Scheme s1. Catalytic asymmetric hydrophosphination of malonate **9**.

A Schlenk tube was charged with Ph₂PH (20.0 mg, 0.107 mmol, 1.0 equiv), catalyst (R)-**1** (3.37 mg, 5.37 µmol, 5 mol%) in solvent (6 mL) and stirred at the stipulated temperature. The substrate **9** (31.9 mg, 0.118 mmol, 1.1 equiv) and NEt₃ (14.9 µL, 0.107 mmol, 1.0 equiv.) was added and stirred. The reaction was monitored for completion by ³¹P{¹H} NMR, then

allowed to warm up to RT and treated with S₈ (6.92 mg, 0.027 mmol, 0.25 equiv.). Volatiles were removed under reduced pressure and the crude product was purified by silica gel column chromatography (1 EA : 15 *n*-hexane) to afford phosphine sulfide **10'** as a white solid in 91% isolated yield. $[\alpha]_D = +10.1$ (*c* 0.68, DCM, Table 1, Entry 7). Mp: 167-168°C. ³¹P{¹H} NMR (CDCl₃, 162 MHz): δ 50.9; ¹H NMR (CDCl₃, 400 MHz): δ 8.34-6.76 (m, 17H, Ar), 5.76 (dd, 1H, *J* = 10.8, 8.2 Hz, CHCOO), 4.98 (dd, 1H, *J* = 12.6, 10.8 Hz, CHP), 3.20 (s, 3H, CH₃), 3.15 (s, 3H, CH₃); ¹³C NMR (CDCl₃, 100 MHz): δ 167.6-167.2 (2C, COO), 133.4-122.6 (22C, Ar), 54.8 (d, 1C, *J* = 4.5 Hz, CH₃), 52.4 (d, 2C, *J* = 7.4 Hz, CH₃), 39.0 (d, 1C, *J* = 50.0 Hz, PCH). The *ee* was determined on a Daicel Chiralpak IC column with *n*-hexane/2-propanol = 95/5, flow = 0.5 mL/min, wavelength = 280 nm. Retention times: 66.8 min (*R*), 76.6 min (*S*).

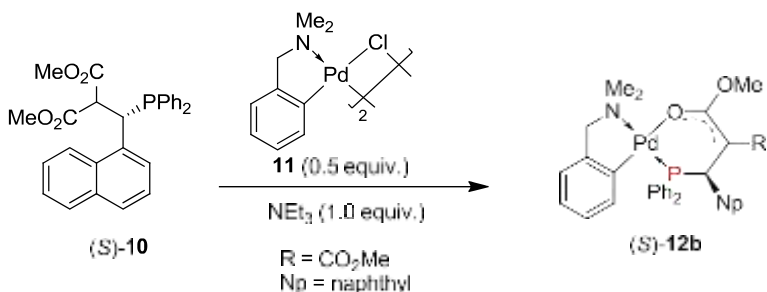
Synthesis of complex (*S*)-**12a**



Scheme s2. Synthesis of coordination complex (*S*)-**12a**.

The volatiles from the crude reaction mixture containing phosphine **10** (1.0 equiv.) were removed under reduced pressure. The residue was redissolved in DCM (10 mL), dimeric complex **11** (0.5 equiv.) was added and stirred at RT for 10 mins. The organic product was extracted with DCM (3 x 50 mL), washed with H₂O (1 x 50 mL), dried over MgSO₄ and filtered. The volatiles were removed by rotary evaporator to afford **12a** as a yellow solid in 99% isolated yield. $[\alpha]_D = -21.9$ (*c* 1.33, DCM). ³¹P{¹H} NMR (CDCl₃, 162 MHz): δ 48.3; ¹H NMR (CDCl₃, 400 MHz): δ 7.96 (d, 1H, *J* = 8.6 Hz, Ar), 7.89 (dd, 2H, *J* = 11.1, 7.5 Hz, Ar), 7.68-7.64 (m, 3H, Ar), 7.45 (dd, 2H, *J* = 9.9, 8.4 Hz, Ar), 7.31-7.17 (m, 6H, Ar), 6.89 (td, 3H, *J* = 8.0, 2.0 Hz, Ar), 6.84 (d, 1H, *J* = 7.0 Hz, Ar), 6.63 (t, 1H, *J* = 7.2 Hz, Ar), 6.15 (t, 1H, *J* = 7.6 Hz, Ar), 6.09 (t, 1H, *J* = 10.6 Hz, PCH), 5.86 (t, 1H, *J* = 7.0 Hz, Ar), 5.53 (t, 1H, *J* = 10.7 Hz, CH(CO₂CH₂)₂), 4.48 (d, 1H, *J* = 13.2 Hz, NCH₂), 3.56 (s, 3H, CO₂CH₃), 3.59 (dd, 1H, *J* = 13.2, 3.4 Hz, NCH₂), 3.07-3.05 (m, 6H, NCH₃), 2.72 (s, 3H, CO₂CH₃); ¹³C NMR (CDCl₃, 100 Hz): δ 169.0 (s, 1C, CO₂CH₃), 168.0 (d, 1C, *J* = 14.9 Hz, CO₂CH₃), 152.2-121.8 (28C, Ar), 73.3 (s, 1C, NCH₂), 56.3 (d, 1C, *J* = 9.2 Hz, CH(CO₂CH₃)₂), 52.8 (s, 1C, CO₂CH₃), 52.0 (s, 1C, CO₂CH₃), 51.4 (s, 1C, NCH₃), 48.9 (s, 1C, NCH₃), 40.2 (d, 1C, *J* = 22.5 Hz, PCH). HRMS (+ESI) m/z: (M + H)⁺ calcd for C₃₇H₃₈ClNO₄PPd, 732.1262; found, 732.1296. Anal. Calcd for C₃₇H₃₇ClNO₄PPd: C, 60.67; H, 5.09; N, 1.91. Found: C, 60.81; H, 5.56; N, 2.00%.

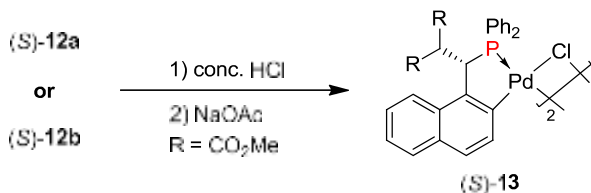
Synthesis of complex (S)-12b



Scheme s3. Synthesis of P-O bidentate complex (S)-12b.

The dimeric complex **11** (0.5 equiv.) was added into the crude reaction mixture containing phosphine **10** (1.0 equiv.) and stirred for 10 mins. The volatiles were removed under reduced pressure to afford the crude residue which on standing overnight, crystallized to form complex **12b** as a yellow block in 75% yield. $[\alpha]_D = -176.8$ (*c* 0.59, DCM). Mp: 121-122°C (dec.). $^{31}\text{P}\{\text{H}\}$ NMR (CDCl_3 , 162 MHz): δ 60.2; ^1H NMR (CDCl_3 , 400 MHz): δ 8.66 (d, 1H, *J* = 7.2 Hz, Ar), 8.31-8.26 (m, 2H, Ar), 7.84 (d, 1H, *J* = 8.7 Hz, Ar), 7.64-7.54 (m, 5H, Ar), 7.44 (t, 1H, *J* = 7.7 Hz, Ar), 7.17 (t, 1H, *J* = 7.4 Hz, Ar), 7.02 (t, 1H, *J* = 7.5 Hz, Ar), 6.94 (d, 1H, *J* = 7.3 Hz, Ar), 6.88 (t, 1H, *J* = 7.5 Hz, Ar), 6.83-6.78 (m, 3H, Ar), 6.63 (td, 2H, *J* = 7.9, 1.9 Hz, Ar), 6.39-6.29 (m, 2H, Ar), 6.33 (d, 1H, *J* = 29.2 Hz, PCH), 4.43 (d, 1H, *J* = 13.8 Hz, NCH_2), 3.72 (s, 3H, $\text{CH}_3\text{O}_2\text{C}$), 3.67 (dd, 1H, *J* = 13.9, 3.3 Hz, NCH_2), 3.56 (s, 3H, $\text{CH}_3\text{O}_2\text{C}$), 3.09 (d, 3H, *J* = 2.9 Hz, NCH_3), 2.83 (s, 3H, NCH_3); ^{13}C NMR (CDCl_3 , 100 MHz): δ 172.2 (d, *J* = 2.4 Hz, 1C, CO_2CH_3), 169.7 (d, *J* = 7.5 Hz, 1C, CO_2CH_3), 148.4-122.4 (29C, Ar), 71.1 (d, 1C, *J* = 2.9 Hz, NCH_2), 51.7 (s, 1C, CH_3CO_2), 50.5 (s, 1C, CH_3CO_2), 49.8 (d, 1C, *J* = 2.2 Hz, NCH_3), 48.8 (d, 1C, *J* = 2.4 Hz, NCH_3), 36.5 (d, 1C, *J* = 29.2 Hz, PCH). HRMS (+ESI) m/z: ($M + H$)⁺ calcd for $\text{C}_{37}\text{H}_{37}\text{NO}_4\text{PPd}$, 696.1495; found, 696.1514.

Synthesis of dimeric complex (S)-13

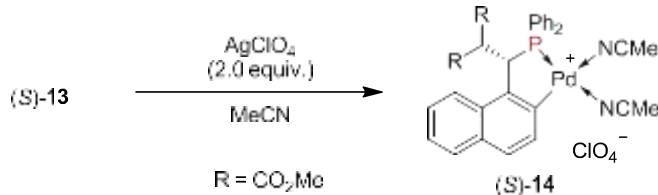


Scheme s4. Synthesis of dimeric complex (S)-13.

The complex **12a** (0.10 g, 136.5 μmol) or **12b** (0.10 g, 143.2 μmol), conc. HCl (0.6 mL) in acetone (6 mL) was refluxed for 90 mins. The solvent was removed, and the residue was extracted with DCM (3 x 25 mL), washed with H_2O (1 x 25 mL), dried over MgSO_4 and filtered. The volatiles were removed under reduced pressure. The crude residue and NaOAc (0.40 g) was refluxed in EtOH (20 mL) for 30 mins. After removal of the solvent, the organic layer was taken up in DCM (3 x 25 mL), washed with H_2O (1 x 25 mL), dried over MgSO_4 and filtered. The crude product was purified by column chromatography (1 DCM : 1 *n*-hexane) to afford complex **13** as a yellow solid in 92% isolated yield. Recrystallization of complex **13** was achieved from a mixture of DCM/*n*-hexane in 84% yield. $[\alpha]_D = +5.6$ (*c*

0.64, DCM). Mp: 180-181°C (dec.). $^{31}\text{P}\{\text{H}\}$ NMR (CDCl_3 , 162 MHz): δ 62.9, 62.3; ^1H NMR (CDCl_3 , 400 MHz): δ 8.01-7.33 (m, 16H, Ar), 5.69-5.63 (m, 1H, CHCOO), 4.38-4.33 (m, 1H, PCH), 3.2 (s, 3H, CH_3), 2.8 (s, 3H, CH_3); ^{13}C NMR (CDCl_3 , 100 MHz): δ 167.8 (2C, CO_2CH_3), 136.0-124.7 (22C, Ar), 53.4 (s, 2C, CO_2CH_3), 52.2 (d, 1C, $J = 19.0$ Hz, PCH). HRMS (+ESI) m/z: ($M + H$)⁺ calcd for $\text{C}_{56}\text{H}_{49}\text{Cl}_2\text{O}_8\text{P}_2\text{Pd}_2$, 1193.0349; found, 1193.0323.

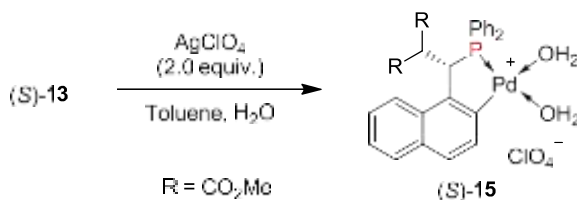
Synthesis of complex (S)-14



Scheme s5. Synthesis of monomeric bisacetonitrile complex (S)-14.

The dimeric complex **13** (0.10 g, 83.7 μmol , 1.0 equiv.) and AgClO_4 (34.7 mg, 167.4 μmol , 2.0 equiv.) in MeCN (10ml) was stirred for 2 h in the dark. The reaction mixture was filtered through celite and the volatiles were removed. Extraction was performed with DCM (3 x 25 mL), the combined organic layer was washed with H_2O (1 x 25 mL), dried over MgSO_4 and filtered. The solvent was removed by rotary evaporator to give complex **14** as a yellow solid in 99% isolated yield. $[\alpha]_D = +357.7$ (*c* 0.15, DCM). Mp: 81-82°C (dec.). $^{31}\text{P}\{\text{H}\}$ NMR (CDCl_3 , 162 MHz): δ 61.5; ^1H NMR (CDCl_3 , 400 MHz): δ 7.97-7.86 (m, 2H, Ar), 7.75-7.65 (m, 4H, Ar), 7.58-7.35 (m, 10H, Ar), 5.68-5.37 (m, 1H, PCH), 4.17 (dd, 1H, $J = 17.6, 9.4$ Hz, $\text{CH}(\text{CO}_2\text{CH}_3)_2$), 3.24 (s, 3H, CO_2CH_3), 2.83 (s, 3H, CO_2CH_3), 2.22 (m, 6H, NCCH₃); ^{13}C NMR (CDCl_3 , 100 MHz): δ 167.2 (s, 1C, CO_2CH_3), 166.8 (d, 1C, $J = 15.0$ Hz, CO_2CH_3), 148.8-123.7 (22C, Ar), 55.3 (d, 1C, $J = 5.6$ Hz, CHCO_2CH_3), 52.3 (d, 2C, $J = 23.7$ Hz, CO_2CH_3), 48.0 (d, 1C, $J = 38.0$ Hz, PCH), 2.5 (s, 2C, NCCH₃). HRMS (+ESI) m/z: ($M + H$)⁺ calcd for $\text{C}_{32}\text{H}_{31}\text{ClN}_2\text{O}_8\text{PPd}$, 743.0541; found, 743.0546.

Synthesis of complex (S)-15

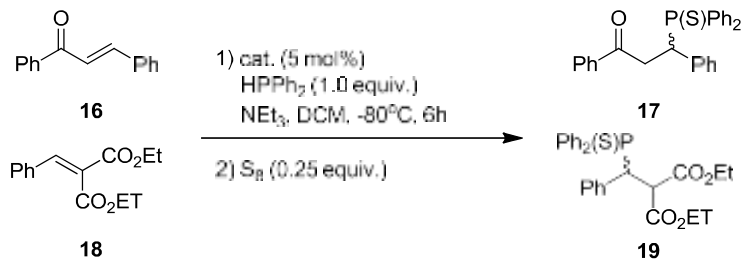


Scheme s6. Synthesis of monomeric bisquo complex (S)-15.

The dimeric complex **13** (0.10 g, 83.7 μmol , 1.0 equiv.) and AgClO_4 (34.7 mg, 167.4 μmol , 2.0 equiv.) in toluene (10ml) and H_2O (1 mL) was stirred for 12 h in the dark. The reaction mixture was filtered through celite and the volatiles were removed. Extraction was performed with DCM (3 x 25 mL), the combined organic layer was washed with H_2O (1 x 25 mL), dried over MgSO_4 and filtered. The solvent was removed by rotary evaporator to give complex **15** as a white solid. Recrystallization of complex **15** was achieved from a mixture of DCM/*n*-hexane to afford (S)-**15** in 75% isolated yield. $[\alpha]_D = +223.0$ (*c* 0.85, DCM). $^{31}\text{P}\{\text{H}\}$ NMR

(CDCl₃, 162 MHz): δ 63.6; ¹H NMR (CDCl₃, 400 MHz): δ 7.89-7.83 (m, 3H, Ar), 7.76-7.71 (m, 3H, Ar), 7.58-7.32 (m, 10H, Ar), 5.54 (dd, 1H, J = 13.4, 9.8 Hz, PCH), 4.34 (dd, 1H, J = 18.0, 9.7 Hz, CH(CO₂CH₃)₂), 3.82 (brs, 4H, OH₂), 3.27 (s, 3H, CO₂CH₃), 2.98 (s, 3H, CO₂CH₃); ¹³C NMR (CDCl₃, 100 MHz): δ 167.2 (s, 2C, CO₂CH₃), 135.5-124.6 (22C, Ar), 56.0 (d, 1C, J = 7.2 Hz, CH(CO₂CH₃)₂), 54.0 (s, 1C, CO₂CH₃), 52.9 (s, 1C, CO₂CH₃), 47.6 (d, 1C, J = 39.2 Hz, PCH). HRMS (+ESI) m/z: (M + H)⁺ calcd for C₂₈H₂₉ClO₁₀PPd, 697.0222; found, 697.0231.

General procedure for asymmetric hydrophosphination of substrates **16** and **18**



Scheme s7. Catalytic asymmetric hydrophosphination of substrates **16** and **18**.

The catalyst (5.37 μ mol, 5 mol %), substrate **16** or **18** (0.118 mmol, 1.1 equiv.) and NEt₃ (14.9 μ L, 0.107 mmol, 1.0 equiv.) was added to a solution of Ph₂PH (20.0 mg, 0.107 mmol, 1.0 equiv) in DCM (6 mL) and stirred at -80°C. The completion of reaction was determined by the disappearance of the signal belonging to HPPh₂ (-40.0 ppm) on ³¹P{¹H} NMR spectroscopy. The crude reaction mixture was treated with S₈ (6.92 mg, 0.027 mmol, 0.25 equiv.) for 10 min to form the respective products. The volatiles were removed under reduced pressure and the crude product was directly loaded onto silica gel column (1 EA : 15 n-hexane) to afford the product **17** as a white solid in quantitative yields. The spectroscopic data obtained for product **17** is consistent with literature.⁵ The ee was determined on a Daicel Chiralpak IC column with n-hexane/2-propanol = 98/2, flow = 0.3 mL/min, wavelength = 270 nm. Retention times: 40.8 min ((S)-**17**), 56.3 min ((R)-**17**). The product **19** was purified by silica gel column (1 EA : 30 n-hexane) and obtained as a white solid in quantitative yields. $[\alpha]_D$ = -62.0 (*c* 0.27, DCM). Mp: 107-108°C. ³¹P{¹H} NMR (CDCl₃, 162 MHz): δ 50.6; ¹H NMR (CDCl₃, 400 MHz): δ 8.23-8.20 (m, 2H, Ar), 7.60-7.50 (m, 5H, Ar), 7.27-7.03 (m, 8H, Ar), 4.86-4.80 (m, 2H, CO₂CH₂), 3.82-3.74 (m, 2H, CO₂CH₂), 3.66-3.57 (m, 1H, PCH), 3.47-3.41 (m, 1H, CH(CO₂CH₂CH₃)₂), 1.01 (t, 3H, J = 7.1 Hz, CH₂CH₃), 0.82 (t, 3H, J = 7.1 Hz, CH₂CH₃). ¹³C NMR (CDCl₃, 100 MHz): δ 166.9 (s, 1C, O=COEt), 166.7 (s, 1C, O=COEt), 133.5-127.3 (m, 15C, Ar), 61.4 (d, 2C, J = 14.3 Hz, CH₂), 53.8 (d, 1C, J = 4.3 Hz, CHPPPh₂), 45.8 (d, 1C, J = 49.3 Hz, CHCOO), 13.3 (d, 2C, J = 11.9 Hz, CH₃). The ee was determined on a Daicel Chiralpak IC column with n-hexane/2-propanol = 98/2, flow = 1.0 mL/min, wavelength = 250 nm. Retention times: 31.4 min, 36.8 min.

Synthesis of gold(I)-phosphine complex (S)-20.



Scheme s8. Synthesis of gold(I)-phosphine complex (*S*)-20.

A mixture of chloro(dimethylsulfide)gold(I) chloride (29.5 mg, 0.10 mmol, 1.0 equiv.) and the phosphine ligand (*S*-**10** (43.8 mg, 0.10 mmol, 1.0 equiv.) in DCM (20 mL) was stirred at RT for 30 min in the dark. The crude product (*S*-**20**) was purified by silica gel column chromatography (1 EA : 4 *n*-hexane) to afford complex (*S*-**20**) as a white solid in 99% isolated yield. Complex (*S*-**20**) was recrystallized from a mixture of DCM/*n*-hexane. $[\alpha]_D = -33.6$ (*c* 0.76, DCM). Mp: 177-178°C. $^{31}\text{P}^{\{1\text{H}\}}$ NMR (CDCl_3 , 162 MHz): δ 46.9; ^1H NMR (CDCl_3 , 400 MHz): δ 8.11 (ddd, 2H, $J = 12.8, 7.1, 2.2$ Hz, Ar), 7.96 (dd, 2H, $J = 11.9, 7.9$ Hz, Ar), 7.66-7.58 (m, 5H, Ar), 7.42 (d, 1H, $J = 7.7$ Hz, Ar), 7.34-7.29 (m, 2H, Ar), 7.04 (dd, 2H, $J = 12.8, 7.4$ Hz, Ar), 6.92 (dd, 1H, $J = 8.0, 6.3$ Hz, Ar), 6.77 (td, 2H, $J = 7.8, 2.6$ Hz, Ar), 5.70-5.64 (m, 1H, PCH), 4.67 (t, 1H, $J = 11.0$ Hz, $\text{CH}(\text{CO}_2\text{CH}_3)_2$), 3.26 (s, 3H, CO_2CH_3), 3.14 (s, 3H, CO_2CH_3); ^{13}C NMR (CDCl_3 , 100 MHz): δ 167.2 (s, 1C, CO_2), 166.3 (d, 1C, $J = 17.9$ Hz, CO_2), 134.9-122.5 (22C, Ar), 56.5 (d, 1C, $J = 13.3$ Hz, $\text{CH}(\text{CO}_2\text{CH}_3)_2$), 52.6 (d, 2C, $J = 8.2$ Hz, CO_2CH_3), 36.8 (d, 1C, $J = 34.7$ Hz, PCH).

Reference

- (1) Y. Huang, R. J. Chew, Y. Li, S. A. Pullarkat and P.-H. Leung, *Org. Lett.* 2011, **13**, 5862-5865.
 - (2) Y. Huang, S. A. Pullarkat, Y. Li and P.-H. Leung, *Inorg. Chem.* 2012, **51**, 2533-2540.
 - (3) A. C. Cope and E. C. Friedrich, *J. Am. Chem. Soc.* 1968, **90**, 909-913.
 - (4) (a) E. J. Corey and M. Chaykovsky, *J. Am. Chem. Soc.* 1965, **87**, 1353-1364; (b) P. D. Pohlhaus, S. D. Sanders, A. T. Parsons, W. Li and J. S. Johnson, *J. Am. Chem. Soc.* 2008, **130**, 8642-8650; (c) M. Skvorcova, L. Grigorjeva and A. Jirgensons, *Org. Lett.* 2015, **17**, 2902-2904.
 - (5) F. Alonso and Y. Moglie, *Curr. Green Chem.* 2014, **1**, 87-93.

NMR Spectra

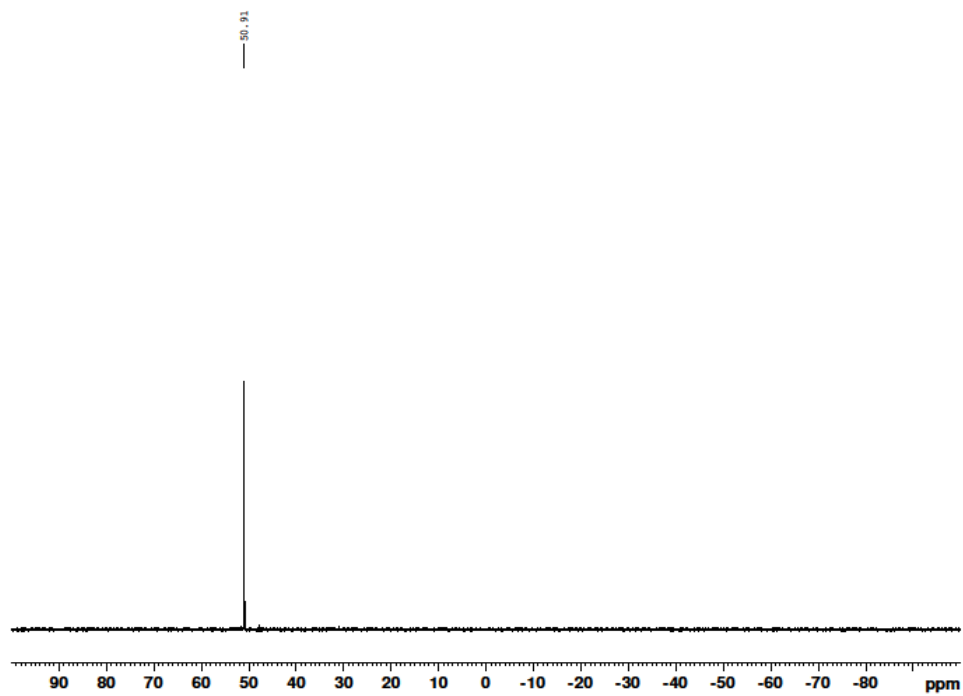


Figure s2. $^{31}\text{P}\{\text{H}\}$ NMR spectrum of phosphine sulfide **10'**.

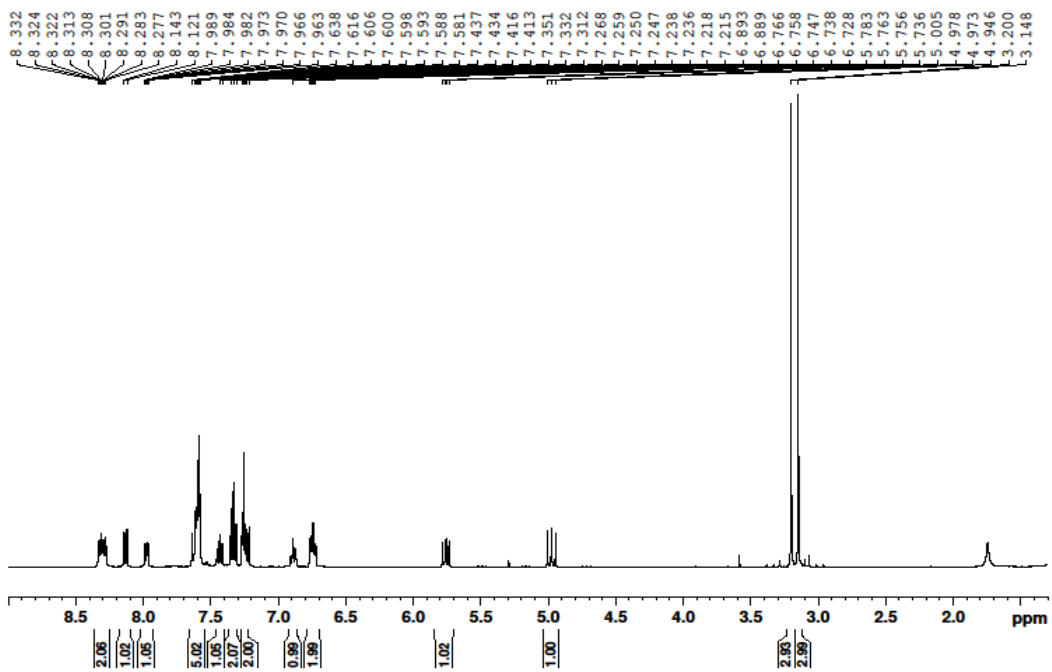


Figure s3. ^1H NMR spectrum of phosphine sulfide **10'**.

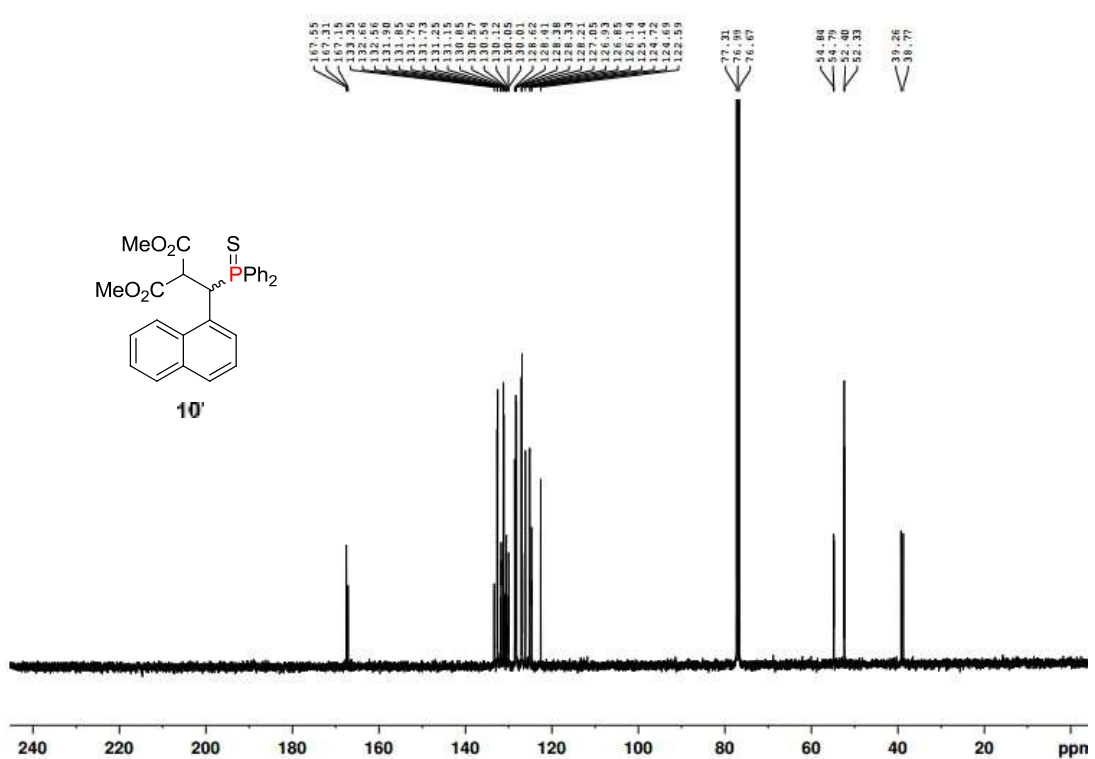


Figure s4. ^{13}C NMR spectrum of phosphine sulfide **10'**.

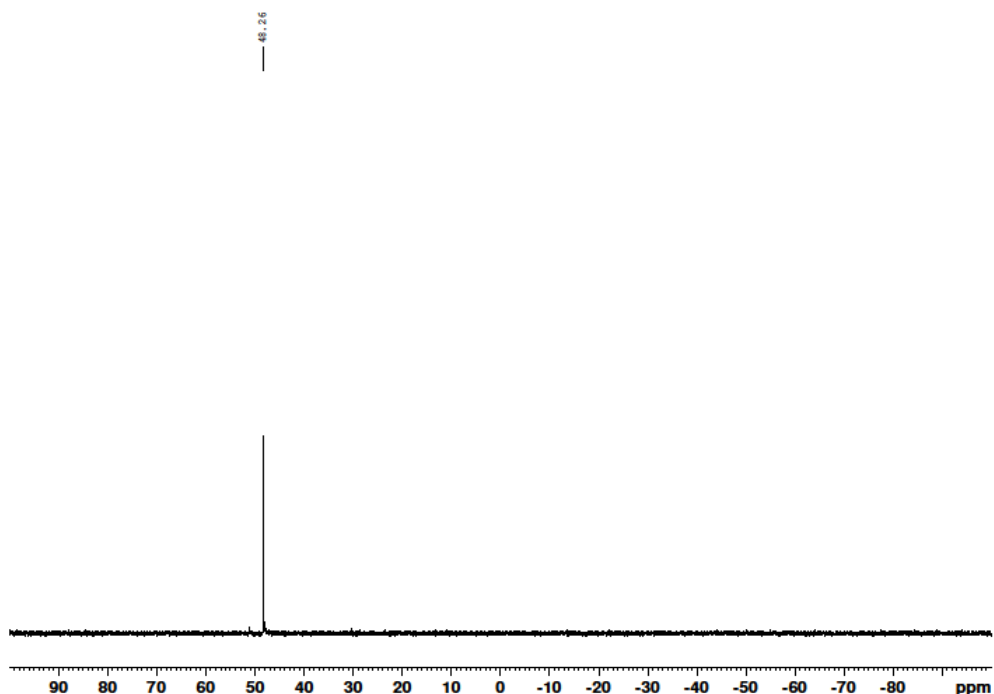


Figure s5. $^{31}\text{P}\{^1\text{H}\}$ NMR spectrum of coordination complex (S)-**12a**.

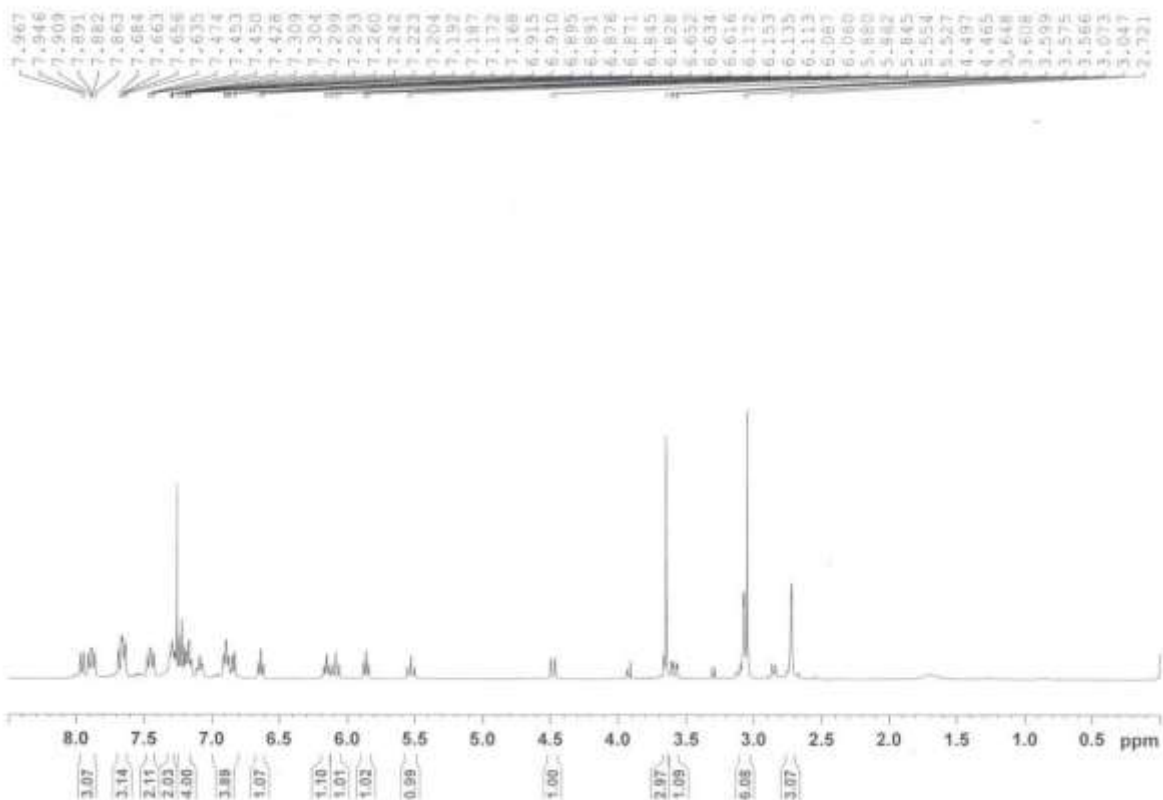


Figure s6. ^1H NMR spectrum of coordination complex (*S*)-**12a**.

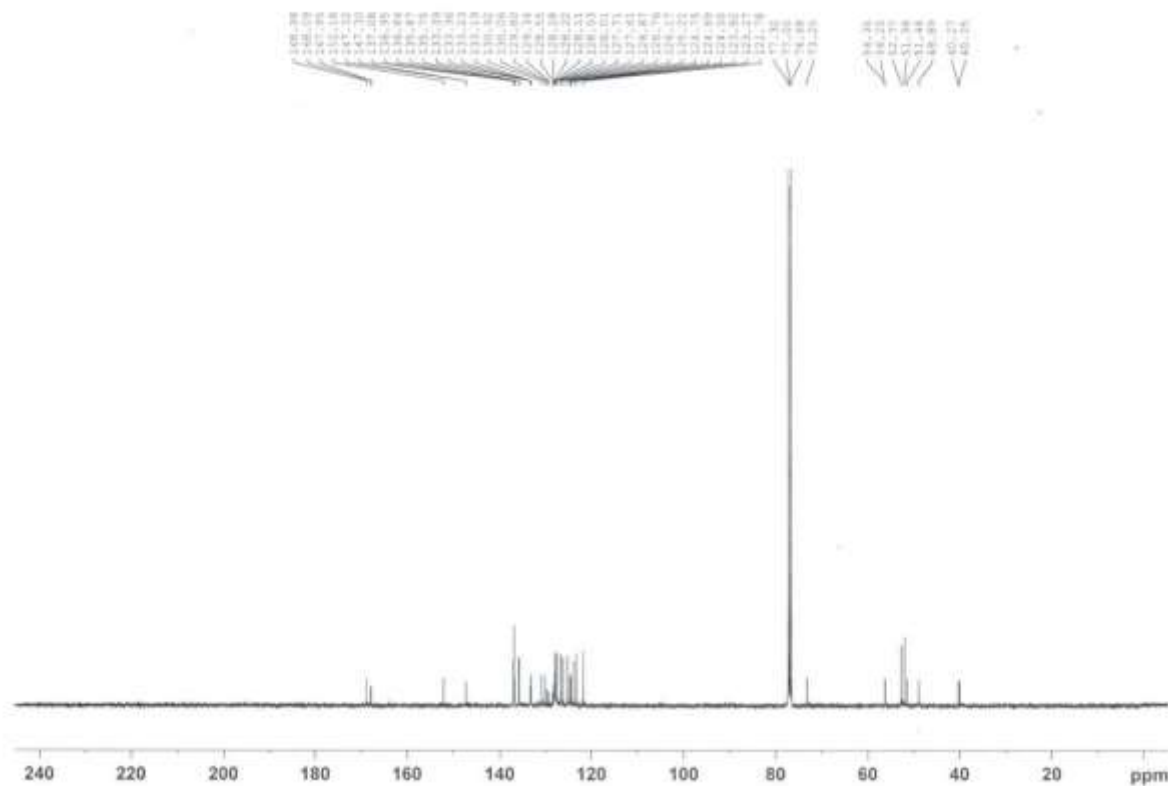


Figure s7. ^{13}C NMR spectrum of coordination complex (*S*)-**12a**.

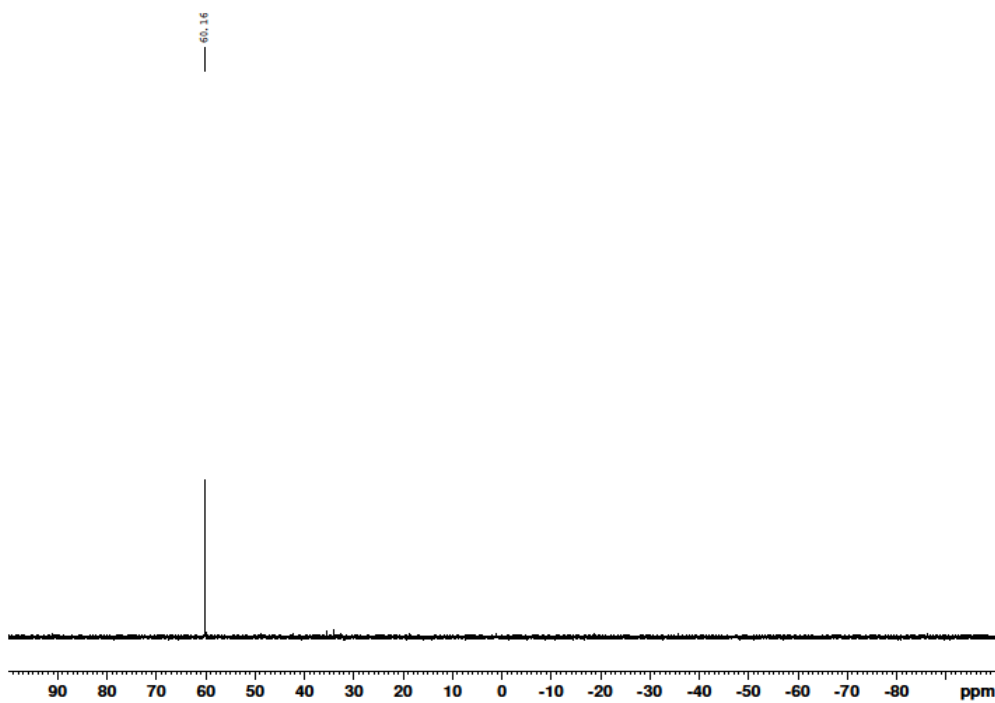


Figure s8. $^{31}\text{P}\{\text{H}\}$ NMR spectrum of P-O bidentate complex (S)-**12b**.

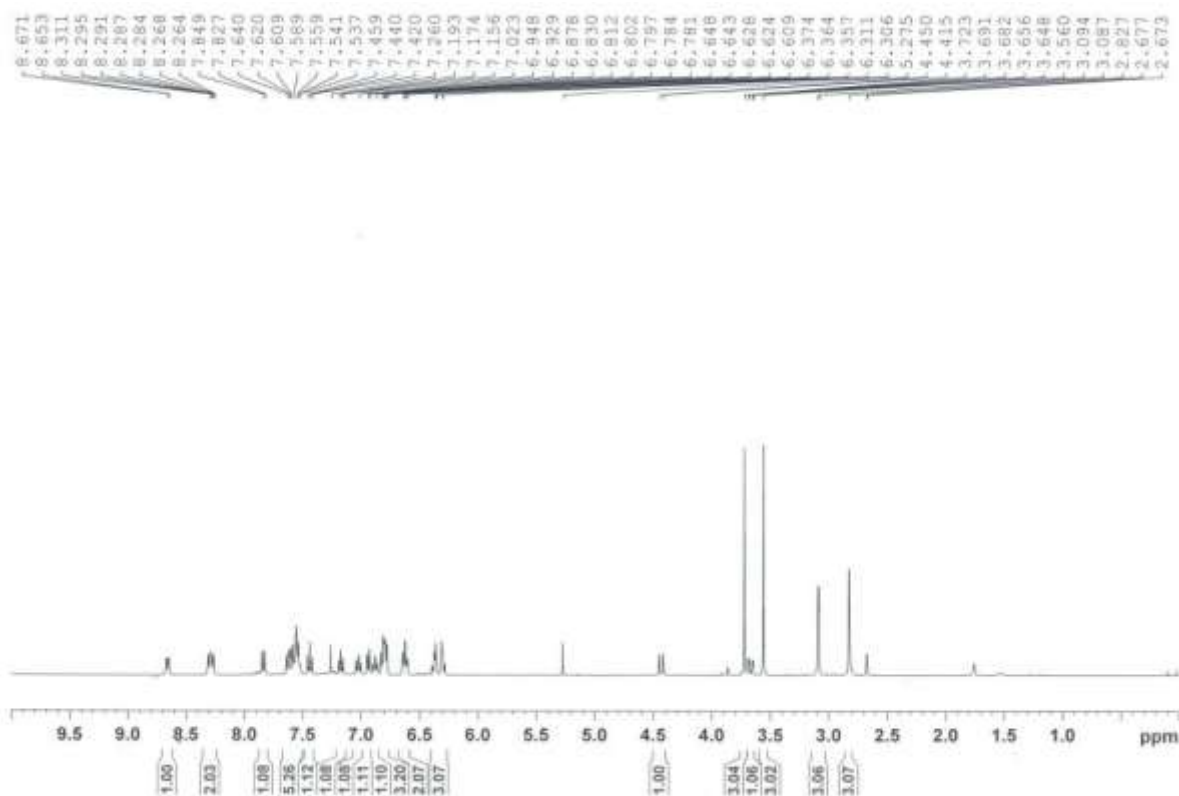


Figure s9. ^1H NMR spectrum of P-O bidentate complex (S)-**12b**.

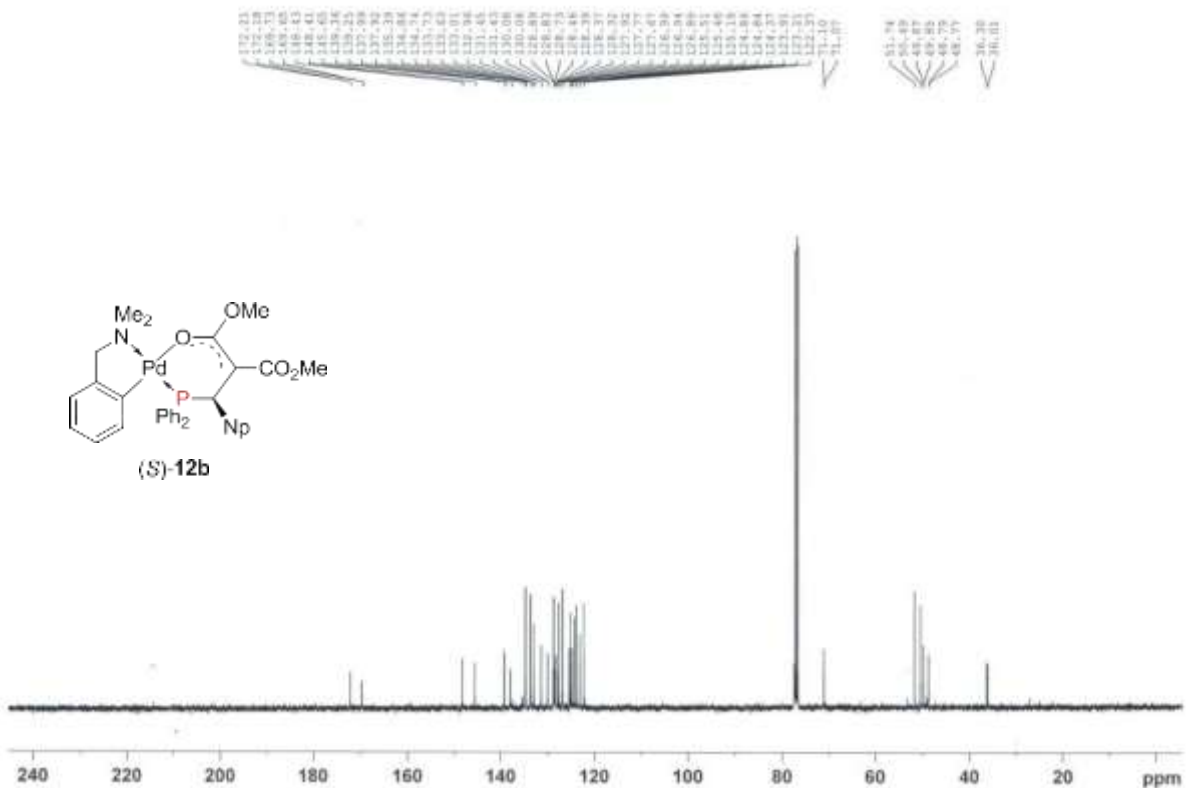


Figure s10. ^{13}C NMR spectrum of P-O bidentate complex (*S*)-**12b**.

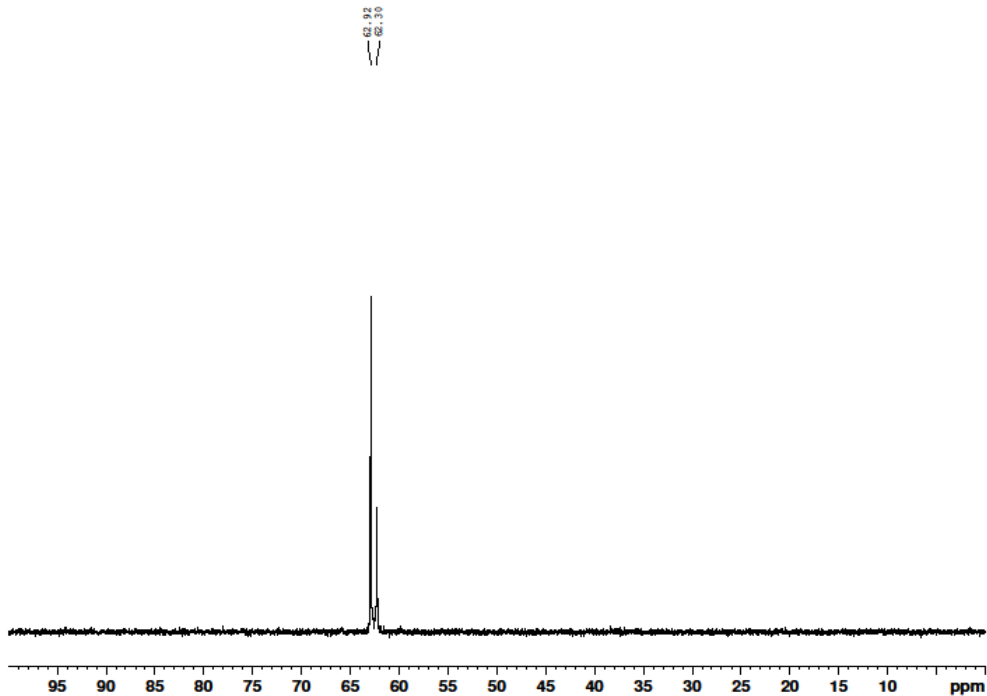


Figure s11. $^{31}\text{P}\{\text{H}\}$ NMR spectrum of dimeric complex (*S*)-13.

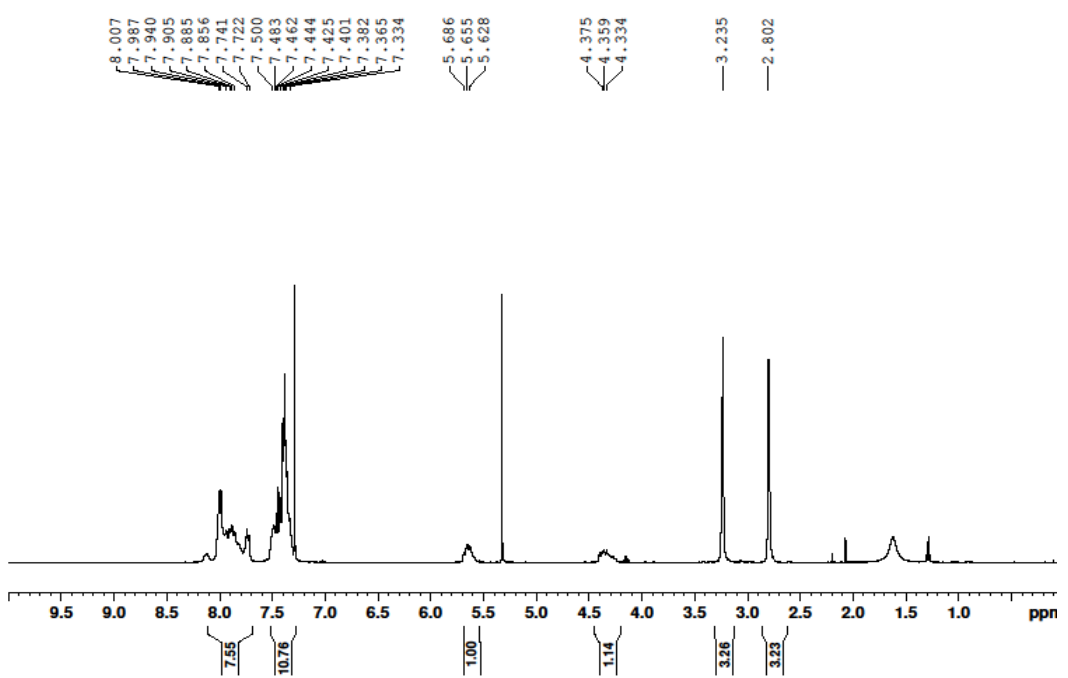


Figure s12. ^1H NMR spectrum of dimeric complex (S)-13.

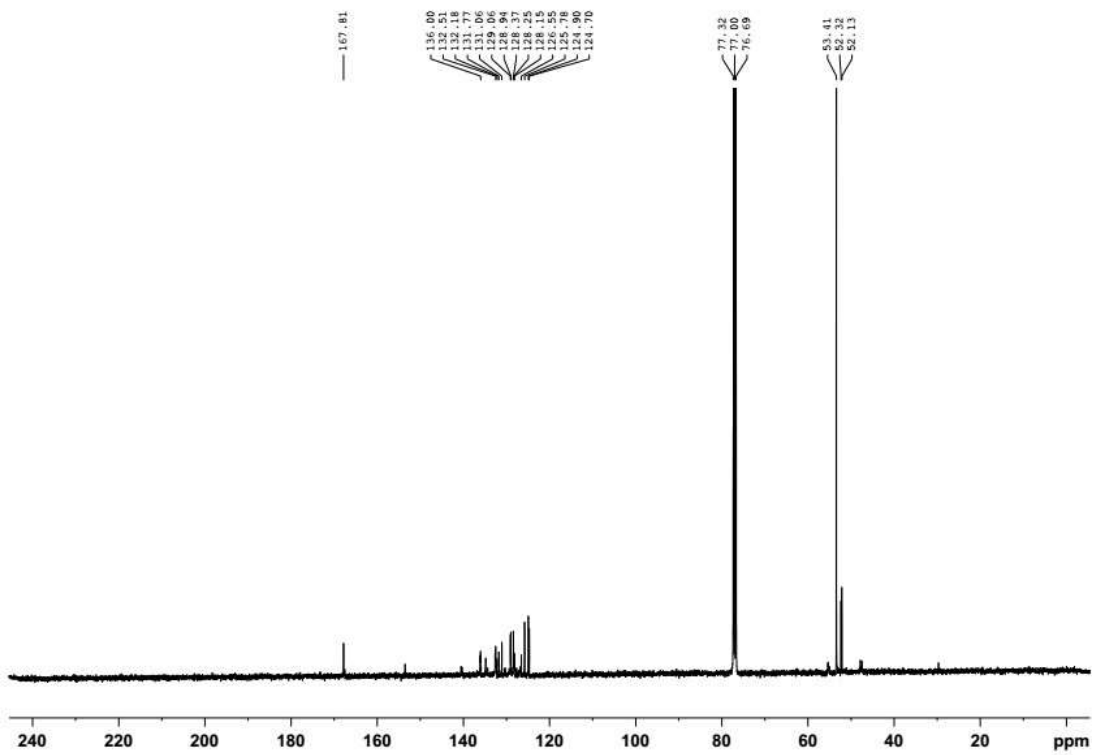


Figure s13. ^{13}C NMR spectrum of dimeric complex (S)-13.

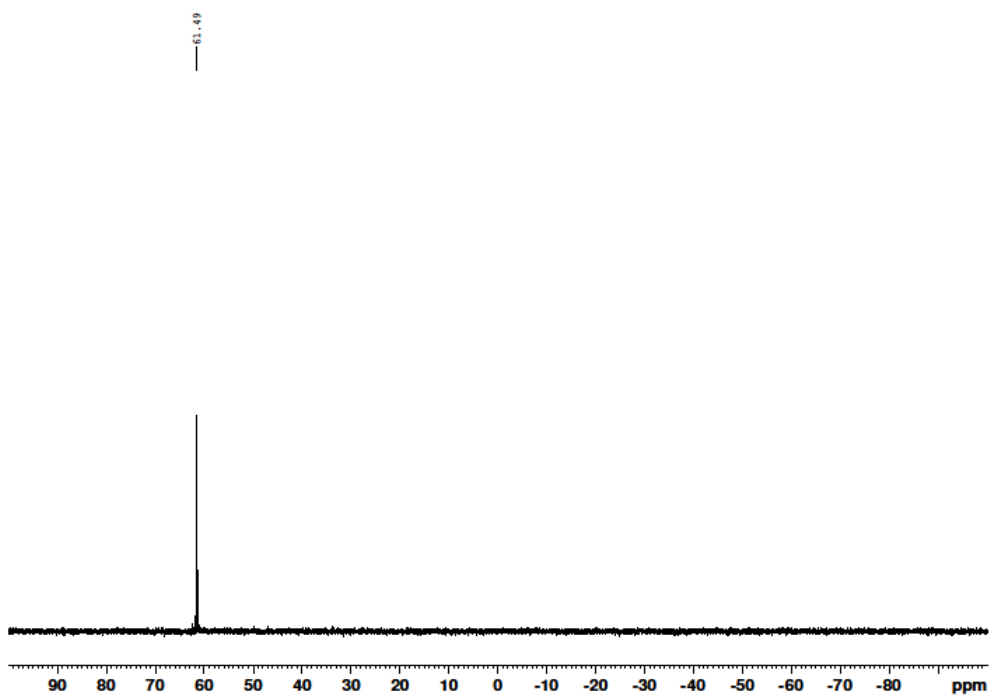


Figure s14. $^{31}\text{P}\{\text{H}\}$ NMR spectrum of monomeric bisacetonitrile complex (*S*)-14.

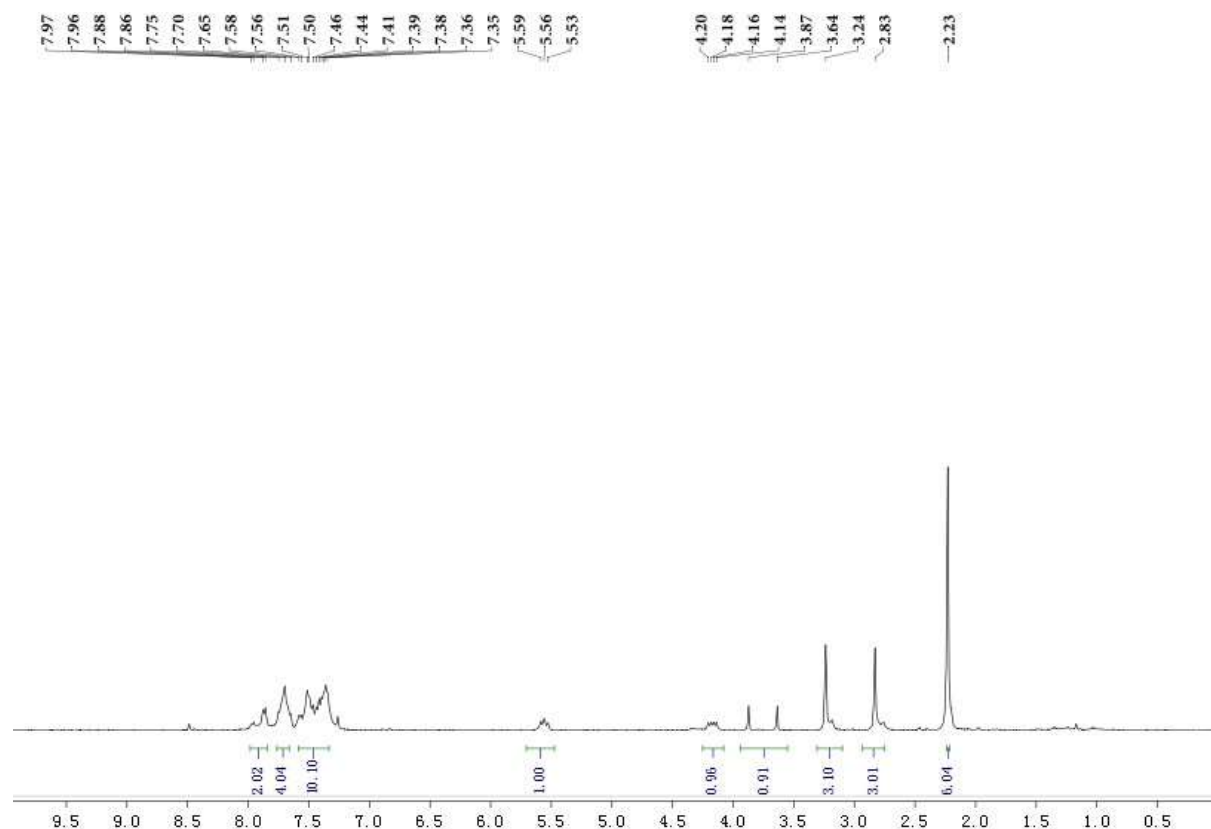


Figure s15. ^1H NMR spectrum of monomeric bisacetonitrile complex (*S*)-14.

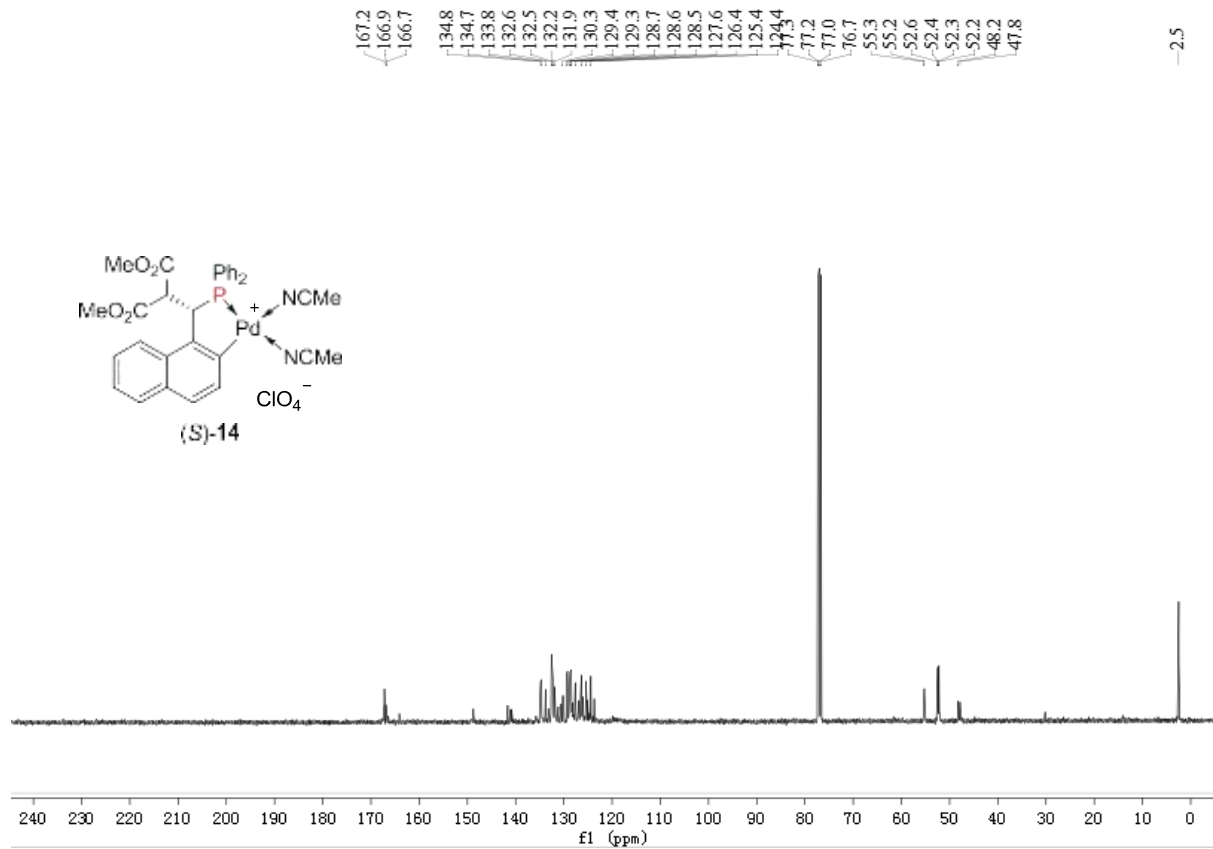


Figure s16. ^{13}C NMR spectrum of monomeric bisacetonitrile complex $(S)\text{-14}$.

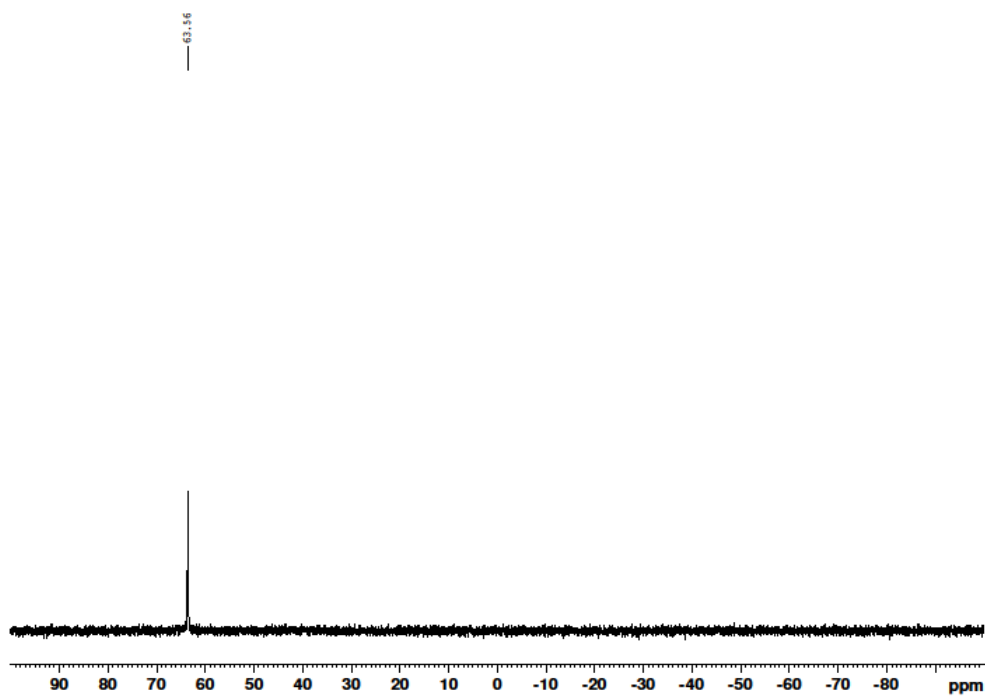


Figure s17. $^{31}\text{P}\{^1\text{H}\}$ NMR spectrum of monomeric bisquo complex $(S)\text{-15}$.

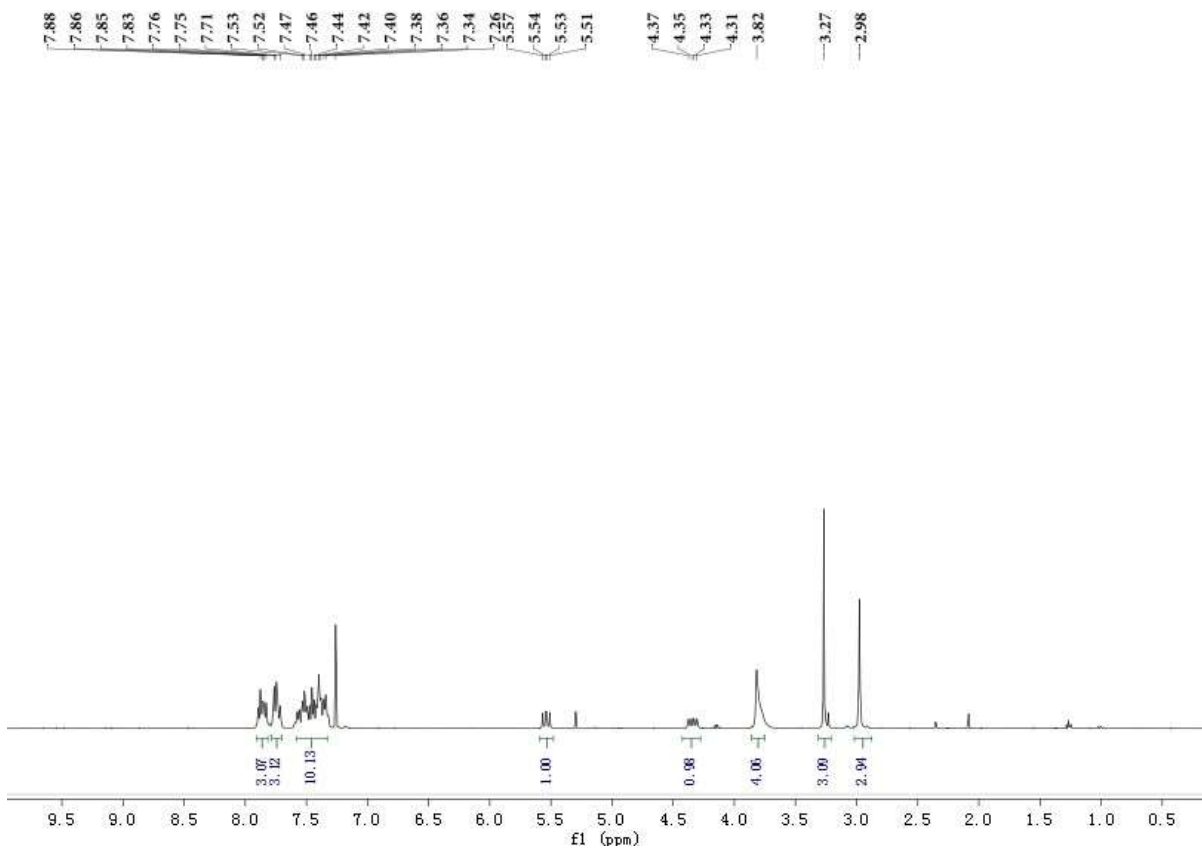


Figure s18. ^1H NMR spectrum of monomeric bis aquo complex (*S*)-**15**.

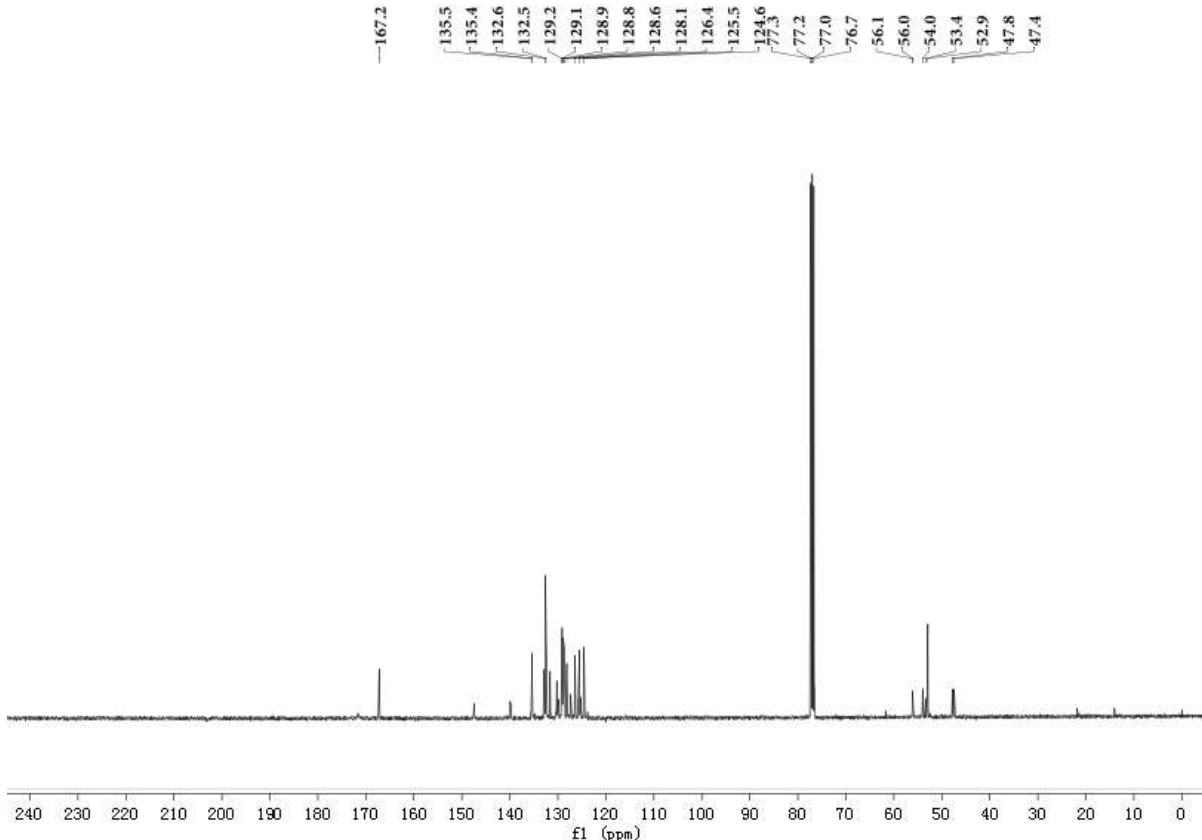


Figure s19. ^{13}C NMR spectrum of monomeric bis aquo complex (*S*)-**15**.

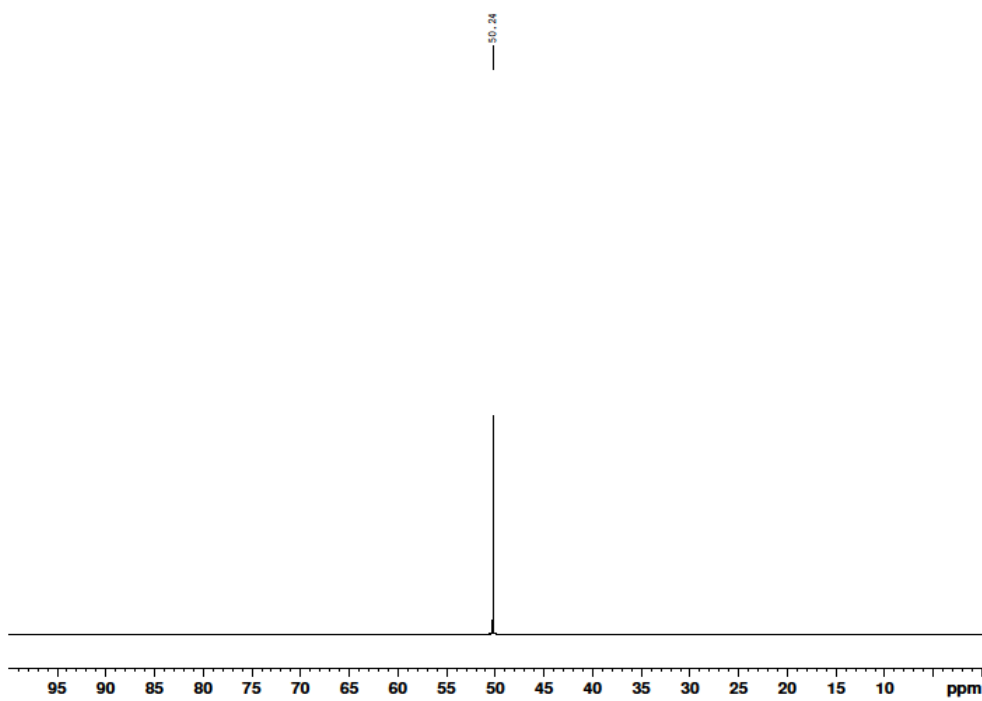


Figure s20. $^{31}\text{P}\{\text{H}\}$ NMR spectrum of phosphine sulfide **19**.

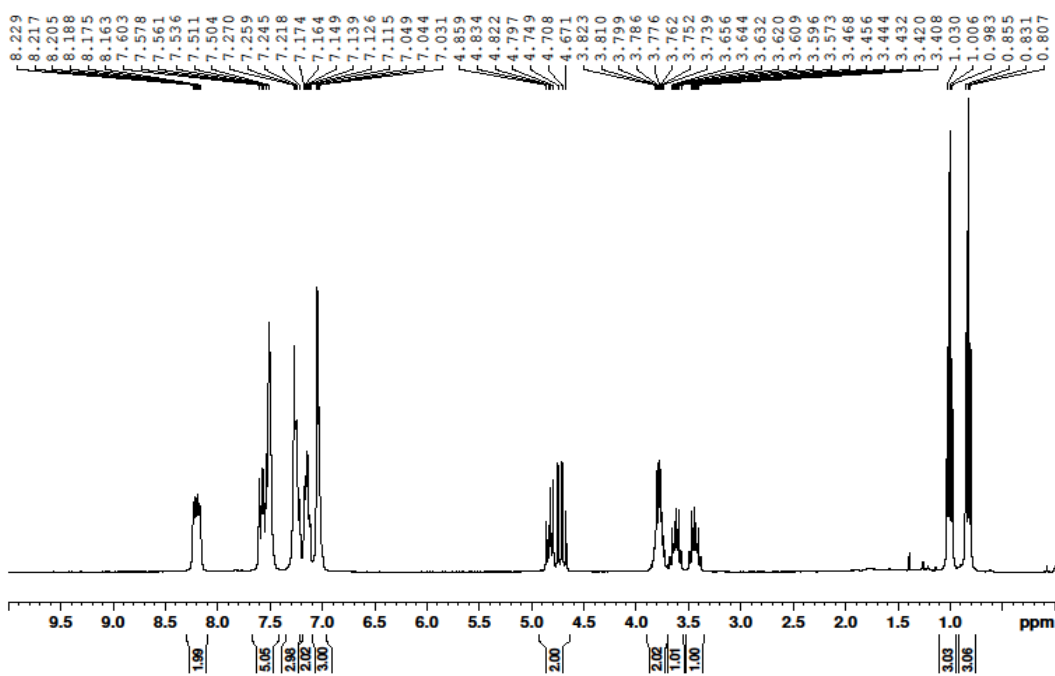


Figure s21. ^1H NMR spectrum of phosphine sulfide **19**.

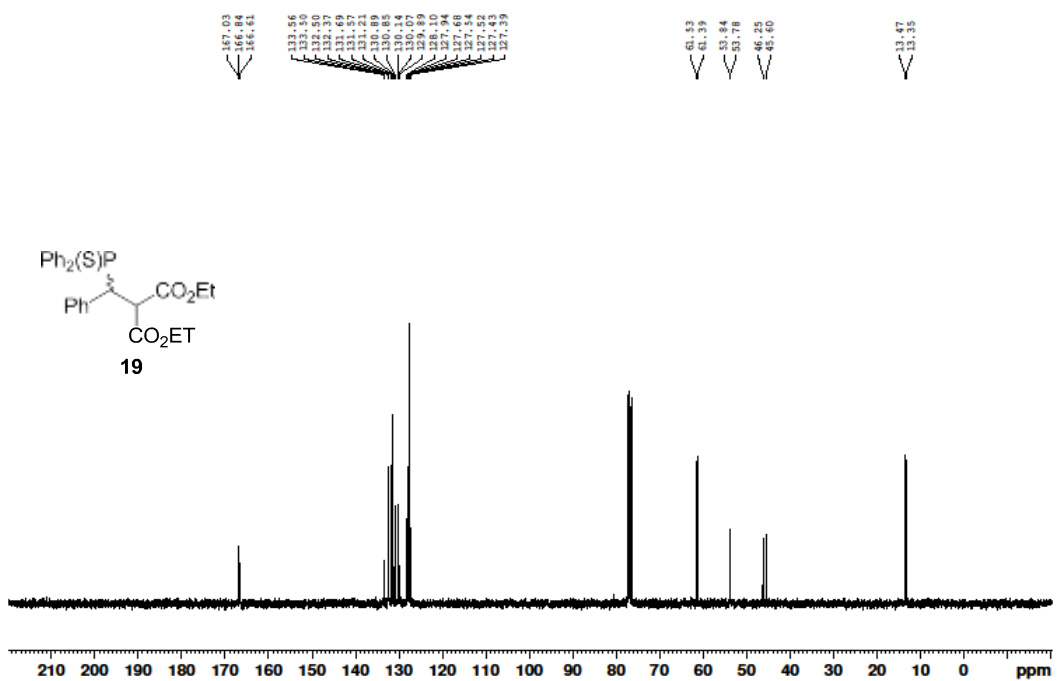


Figure s22. ^{13}C NMR spectrum of phosphine sulfide **19**.

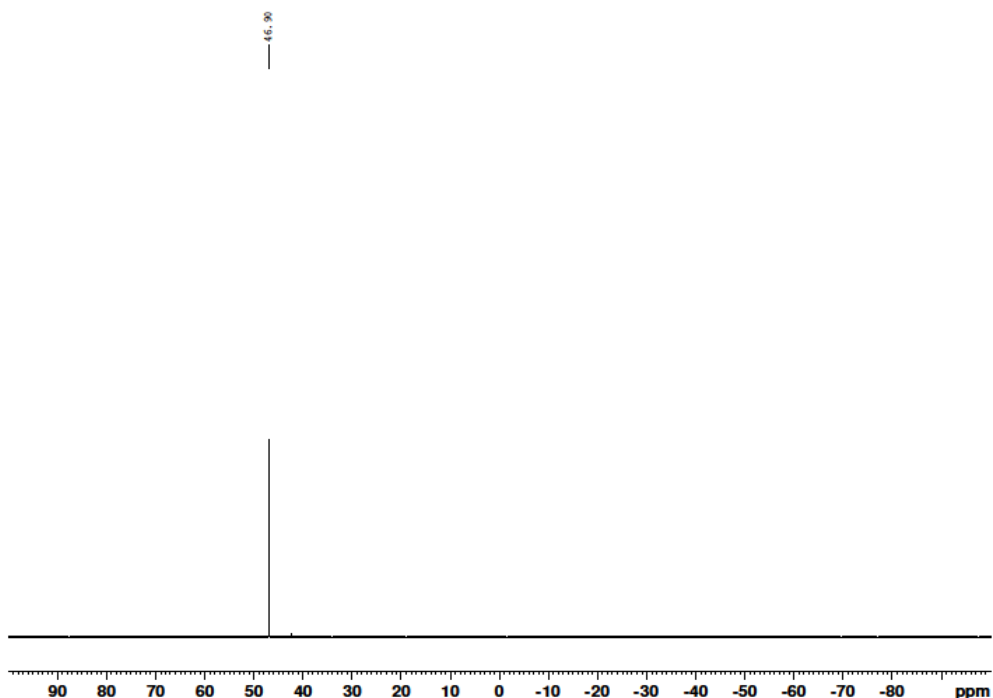


Figure s23. $^{31}\text{P}\{^1\text{H}\}$ NMR spectrum of phosphine gold(I) complex (S)-**20**.

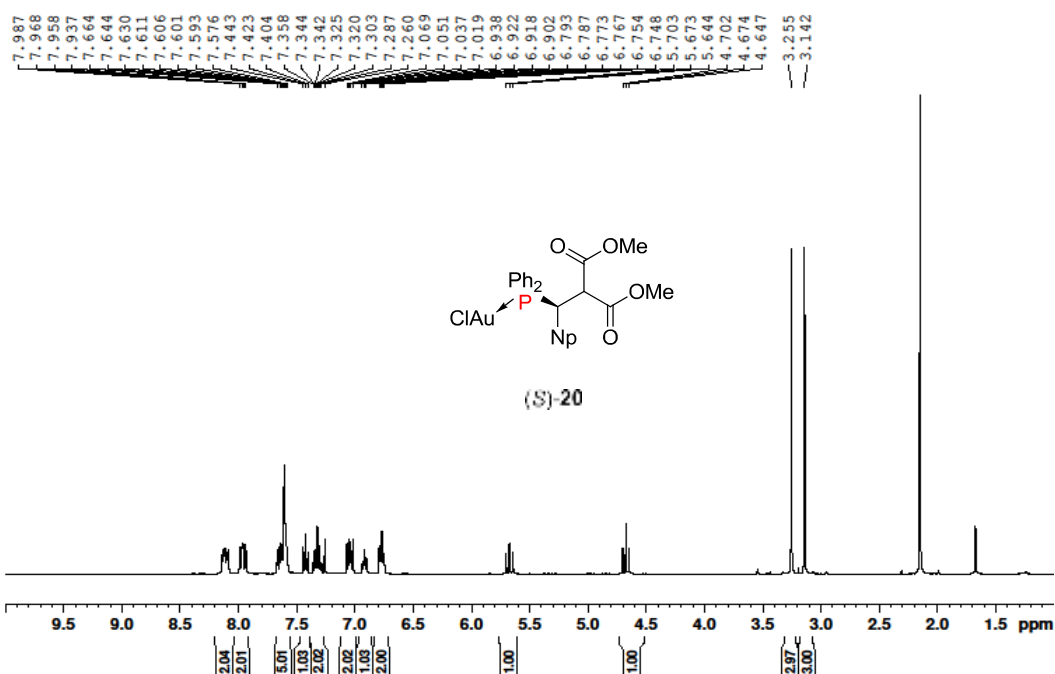


Figure s24. ^1H NMR spectrum of phosphine gold(I) complex $(S)\text{-}20$.

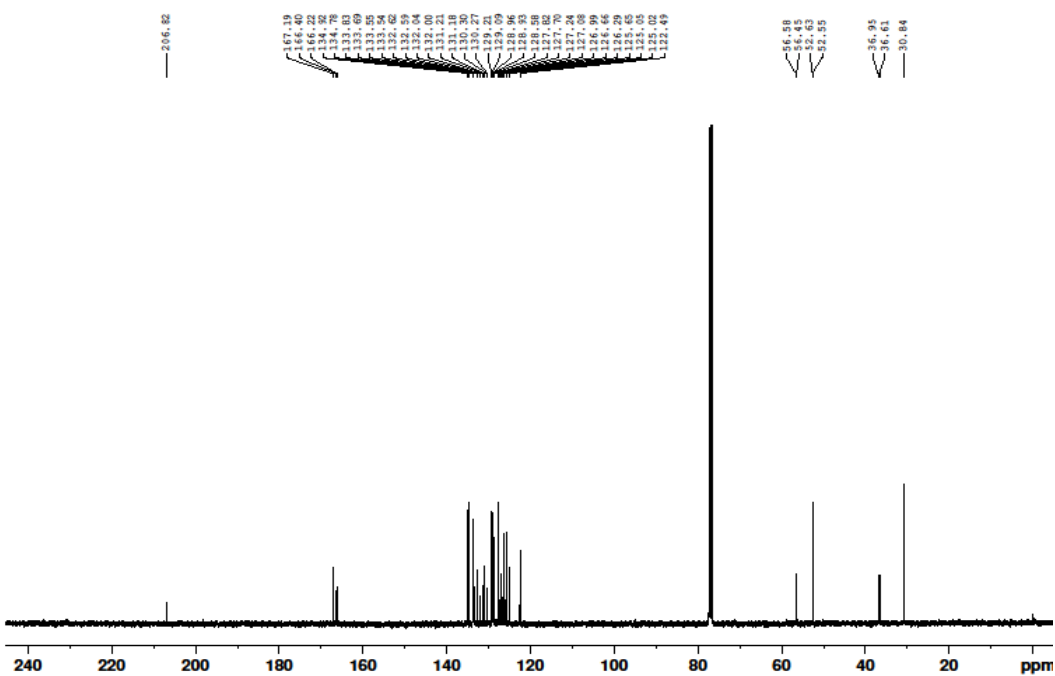


Figure s25. ^{13}C NMR spectrum of phosphine gold(I) complex $(S)\text{-}20$.

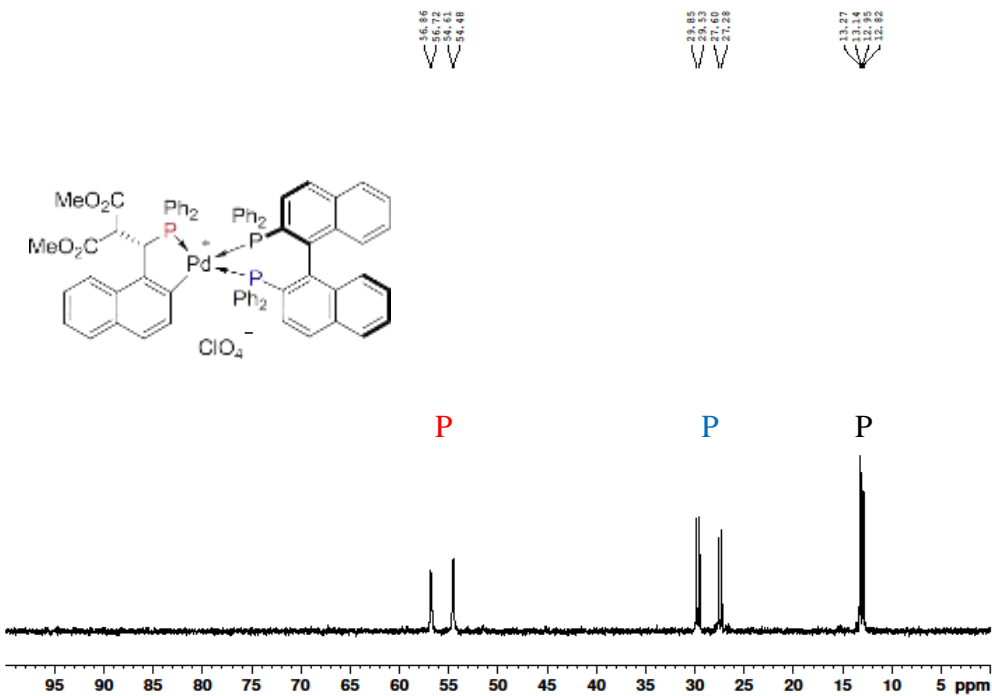
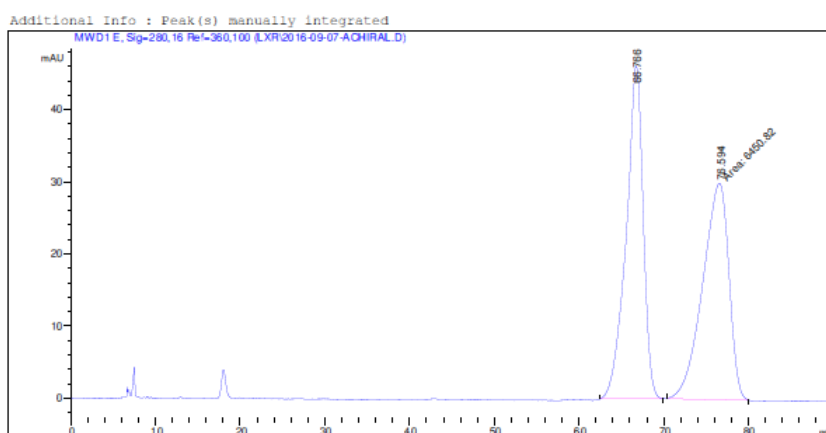


Figure s26. $^{31}\text{P}\{\text{H}\}$ NMR spectrum of product from coordination of (S)-BINAP to complex (S)-14.

From the coordination experiment conducted between complex (S)-14 and (S)-BINAP, the *ee* of the PC-palladacycle complex was determined to be >99% after a single recrystallization. With reference to the $^{31}\text{P}\{\text{H}\}$ NMR spectrum obtained above, the three phosphorus atoms located on the coordination complex may be identified by their coupling constants and chemical shifts. If both enantiomers of the PC-palladacycle complex were present, two sets of similar signals (with different intensities based on the enantiomeric ratio of the isomers) should be obtained. Since that is not observed, it is clear that only one enantiomer of the complex is present after a single recrystallization.

HPLC Spectra



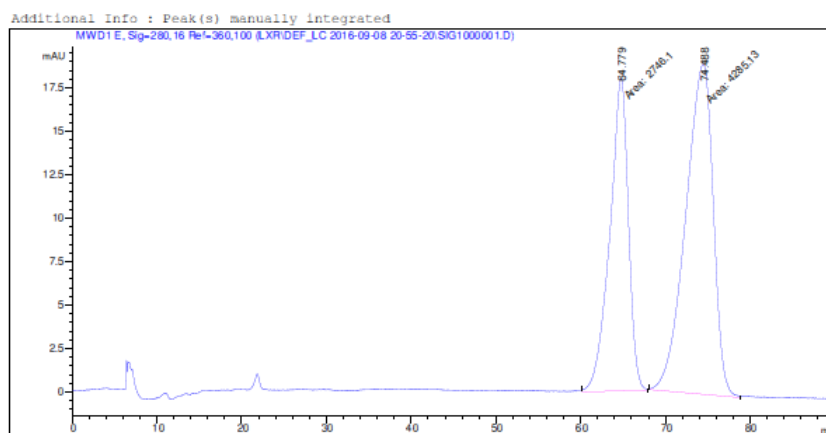
Area Percent Report

Sorted By : Signal
Multiplier: : 1.0000
Dilution: : 1.0000
Sample Amount: : 1.00000 [ng/uL] (not used in calc.)
Use Multiplier & Dilution Factor with ISTDs

Signal 1: MWDL E, Sig-280,16 Ref-360,100

Peak #	RetTime [min]	Type	Width [min]	Area [mAU*s]	Height [mAU]	Area %
1	66.766	BB	1.8289	6461.04736	46.10719	50.0396
2	76.594	MM	3.5812	6450.81738	30.02137	49.9604

Figure s27. HPLC spectrum for racemic phosphine sulfide **10'**.



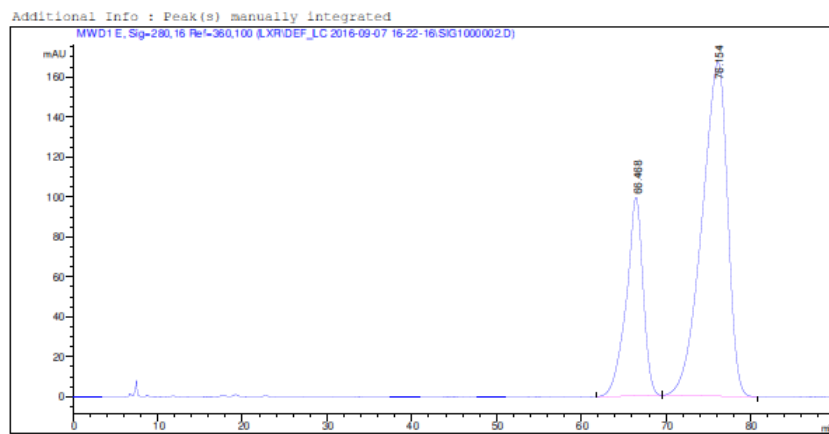
Area Percent Report

Sorted By : Signal
Multiplier: : 1.0000
Dilution: : 1.0000
Use Multiplier & Dilution Factor with ISTDs

Signal 1: MWDL E, Sig-280,16 Ref-360,100

Peak #	RetTime [min]	Type	Width [min]	Area [mAU*s]	Height [mAU]	Area %
1	64.779	MM	2.5462	2746.10034	17.97495	39.0558
2	74.488	MM	3.7599	4285.13086	18.99499	60.9442

Figure s28. HPLC spectrum for phosphine sulfide **10'** in Table 1 Entry 1.



Area Percent Report

Sorted By : Signal
 Multiplier: : 1.0000
 Dilution: : 1.0000
 Use Multiplier & Dilution Factor with ISTDs

Signal 1: MWD1 E, Sig=280,16 Ref=360,100

Peak #	RetTime [min]	Type	Width [min]	Area [mAU*s]	Height [mAU]	Area %
1	66.468	BB	1.8816	1.36759e4	99.36965	28.0082
2	76.154	BB	2.5996	3.51524e4	167.28322	71.9918

Figure s29. HPLC spectrum for phosphine sulfide **10'** in Table 1 Entry 2.

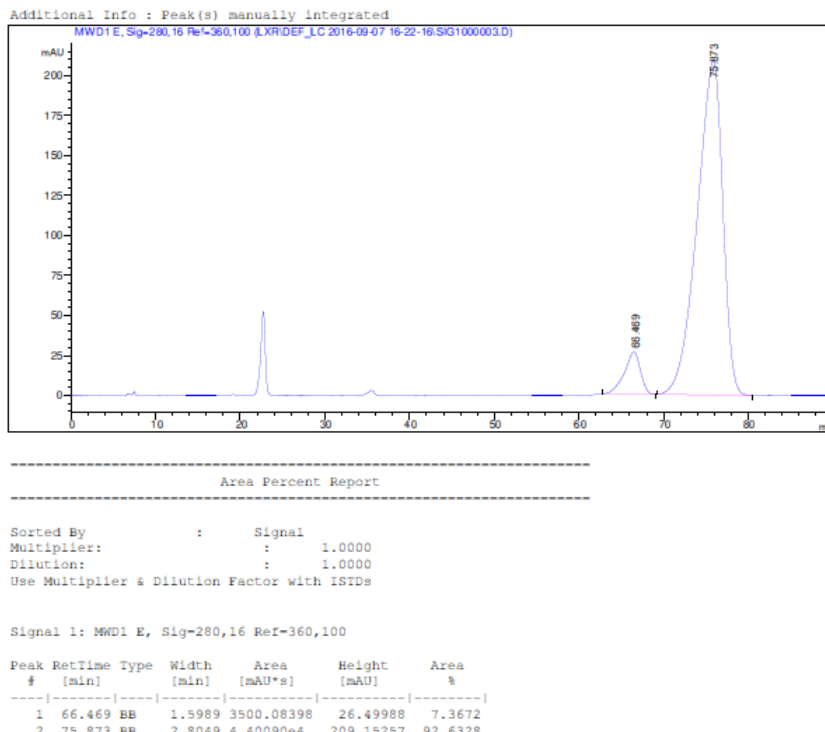
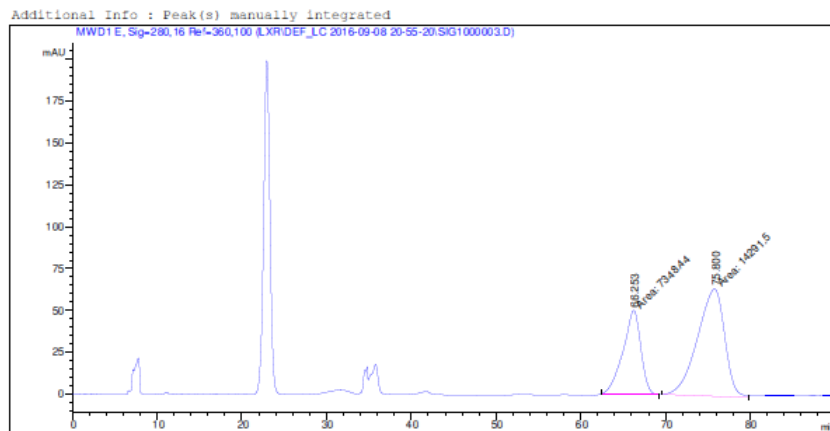


Figure s30. HPLC spectrum for phosphine sulfide **10'** in Table 1 Entry 3.



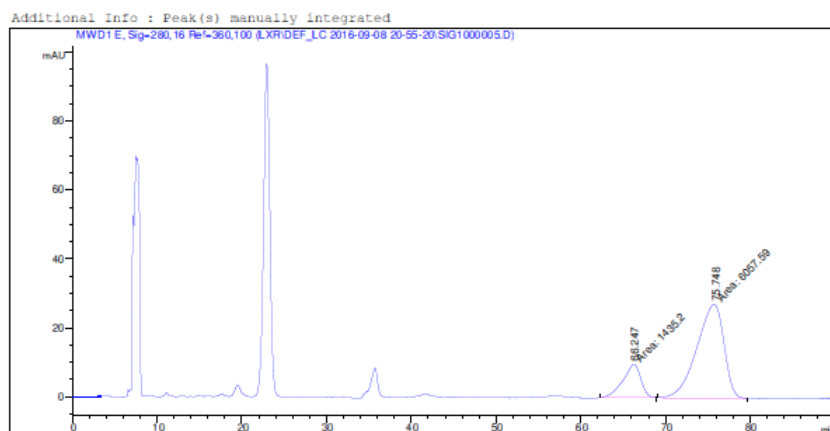
Area Percent Report

Sorted By : Signal
Multiplier: : 1.0000
Dilution: : 1.0000
Use Multiplier & Dilution Factor with ISTDs

Signal 1: MWD1 E, Sig=280,16 Ref=360,100

Peak #	RetTime [min]	Type	Width [min]	Area [mAU*s]	Height [mAU]	Area %
1	66.253	MM	2.4440	7348.43799	50.11135	33.9577
2	75.800	MM	3.7153	1.42915e4	64.11132	66.0423

Figure s31. HPLC spectrum for phosphine sulfide **10'** in Table 1 Entry 4.



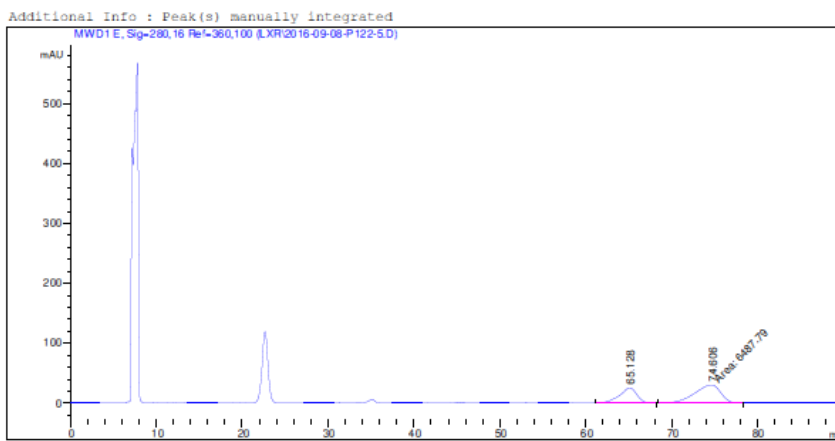
Area Percent Report

Sorted By : Signal
Multiplier: : 1.0000
Dilution: : 1.0000
Use Multiplier & Dilution Factor with ISTDs

Signal 1: MWD1 E, Sig=280,16 Ref=360,100

Peak #	RetTime [min]	Type	Width [min]	Area [mAU*s]	Height [mAU]	Area %
1	66.247	MM	2.4635	1435.19775	9.70981	19.1544
2	75.748	MM	3.7015	6057.59100	27.27573	80.8456

Figure s32. HPLC spectrum for phosphine sulfide **10'** in Table 1 Entry 5.



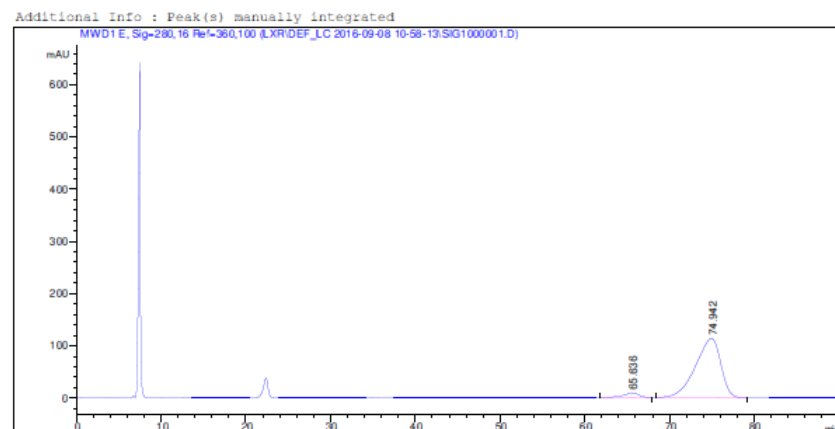
Area Percent Report

```
Sorted By      :      Signal
Multiplier:    :      1.0000
Dilution:     :      1.0000
Sample Amount: :      1.00000 [ng/uL] (not used in calc.)
Use Multiplier & Dilution Factor with ISIDs
```

Signal 1: MWD1 E, Sig-280,16 Ref-360,100

Peak RetTime	Type	Width	Area	Height	Area %
# [min]		[min]	[mAU*s]	[mAU]	
1 65.128	BB	1.6925	3535.75317	25.39251	35.2745
2 74.606	MM	3.5523	6487.79199	30.43944	64.7255

Figure s33. HPLC spectrum for phosphine sulfide **10'** in Table 1 Entry 6.



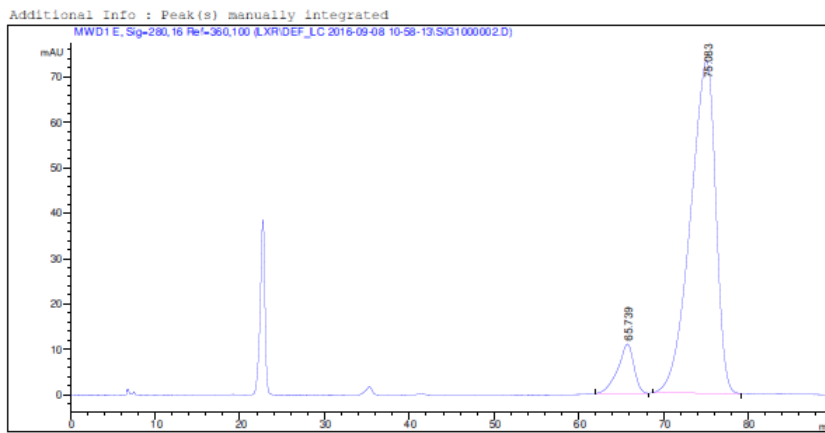
Area Percent Report

```
Sorted By      :      Signal
Multiplier:    :      1.0000
Dilution:     :      1.0000
Use Multiplier & Dilution Factor with ISIDs
```

Signal 1: MWD1 E, Sig-280,16 Ref-360,100

Peak RetTime	Type	Width	Area	Height	Area %
# [min]		[min]	[mAU*s]	[mAU]	
1 65.636	BB	1.5541	1144.09460	8.62197	4.6516
2 74.942	BB	2.4382	2.34516e4	113.42535	95.3484

Figure s34. HPLC spectrum for phosphine sulfide **10'** in Table 1 Entry 7.



Area Percent Report

Sorted By : Signal
Multiplier: : 1.0000
Dilution: : 1.0000
Use Multiplier & Dilution Factor with ISTDs

Signal 1: MWD1 E, Sig=280,16 Ref=360,100

Peak #	RetTime [min]	Type	Width [min]	Area [mAU*s]	Height [mAU]	Area %
1	65.739	BB	1.5539	1428.03503	10.84727	8.5892
2	75.083	BB	2.4571	1.51980e4	73.29485	91.4108

Figure s35. HPLC spectrum for phosphine sulfide **10'** in Table 1 Entry 8.

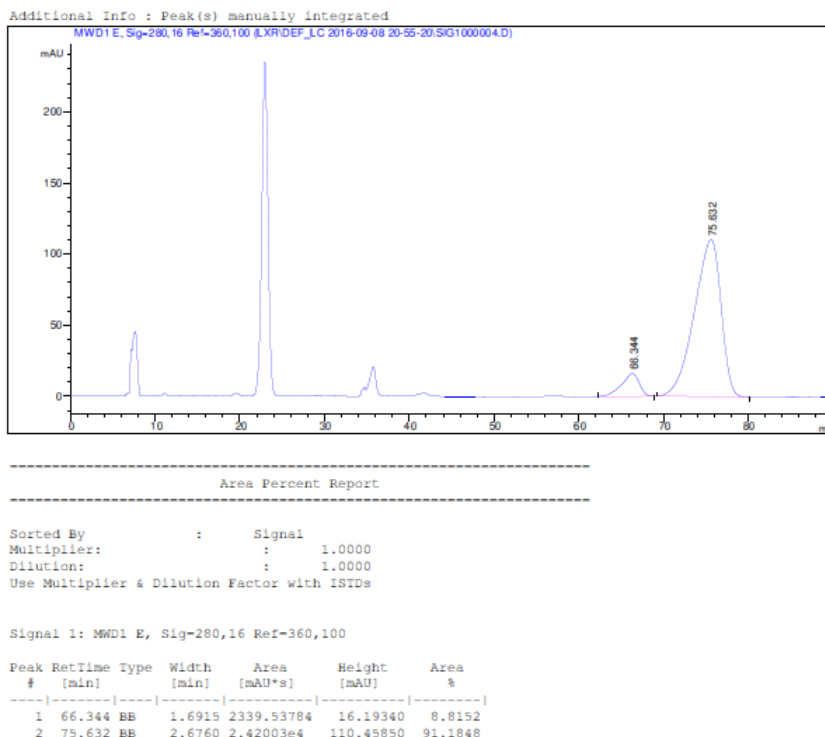
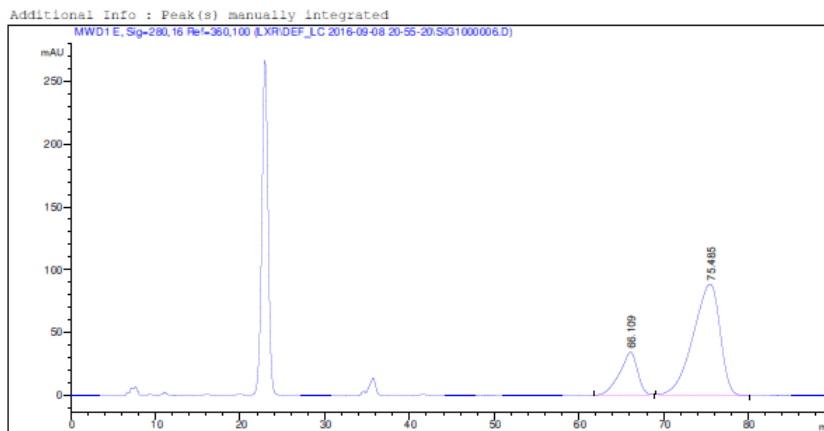


Figure s36. HPLC spectrum for phosphine sulfide **10'** in Table 1 Entry 9.



Area Percent Report

Sorted By : Signal
 Multiplier: : 1.0000
 Dilution: : 1.0000
 Use Multiplier & Dilution Factor with ISTDs

Signal 1: MWD1 E, Sig=280,16 Ref=360,100

Peak #	RetTime [min]	Type	Width [min]	Area [mAU*s]	Height [mAU]	Area %
1	66.109	BB	1.7563	5032.10059	34.08775	20.5084
2	75.485	BB	2.5806	1.95047e4	88.65862	79.4916

Figure s37. HPLC spectrum for phosphine sulfide **10'** in Table 1 Entry 10.

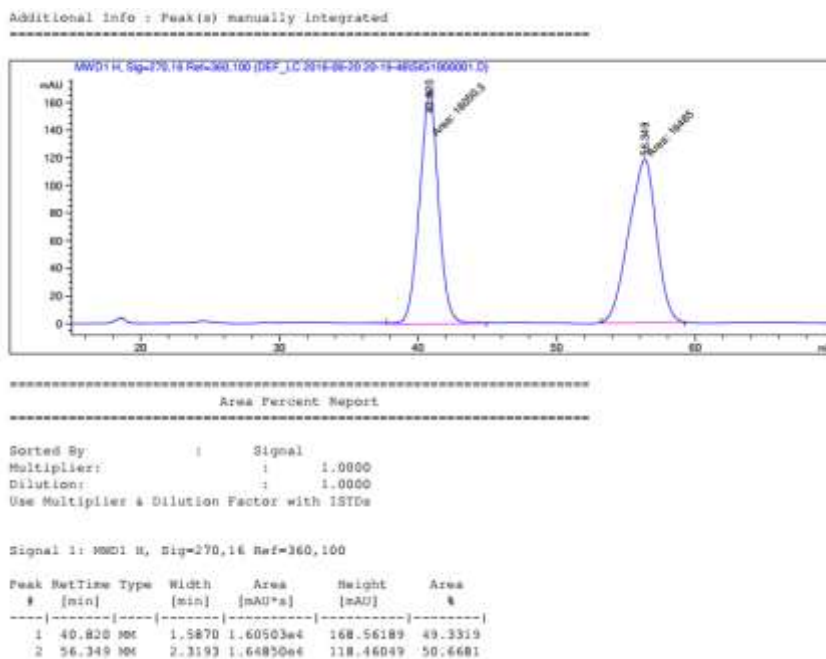
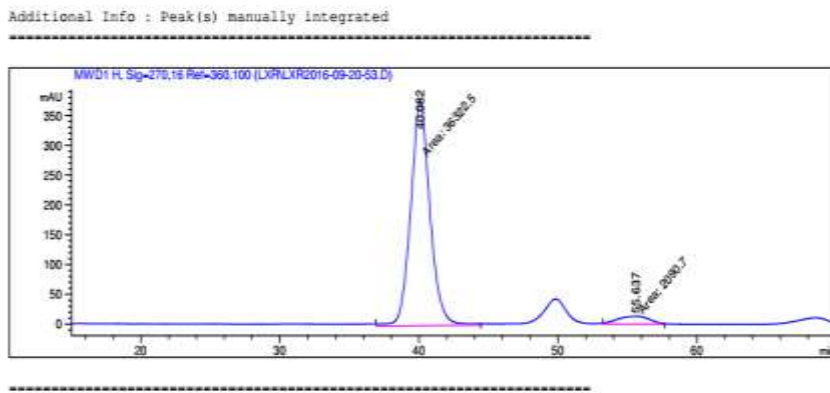


Figure s38. HPLC spectrum for racemic phosphine sulfide **17**.



Area Percent Report

Sorted By : Signal
 Multiplier: : 1.0000
 Dilution: : 1.0000
 Sample Amount: : 1.00000 [ng/uL] (not used in calc.)
 Use Multiplier & Dilution Factor with ISTDs

Signal 1: MWD1 H, Sig=270,16 Ref=360,100

#	RetTime	Type	Width	Area	Height	Area %
	[min]		[min]	[mAU*s]	[mAU]	%
1	40.082	MM	1.6060	3.63225e4	376.95654	94.5573
2	55.637	MM	2.6653	2090.69873	13.07367	5.4427

Figure s39. HPLC spectrum for phosphine sulfide **17** in Table 2 Entry 1.

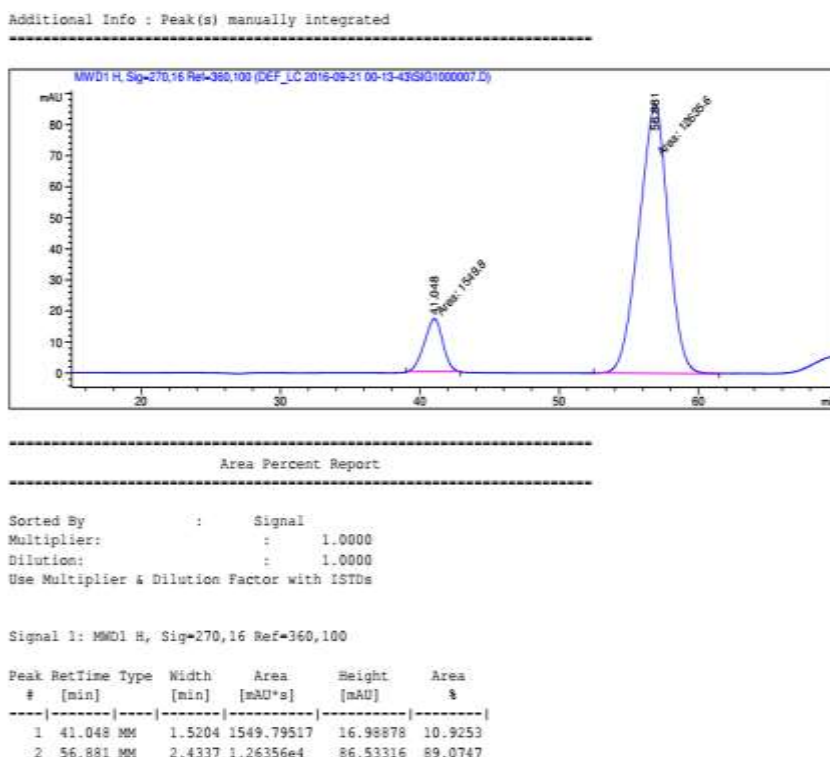
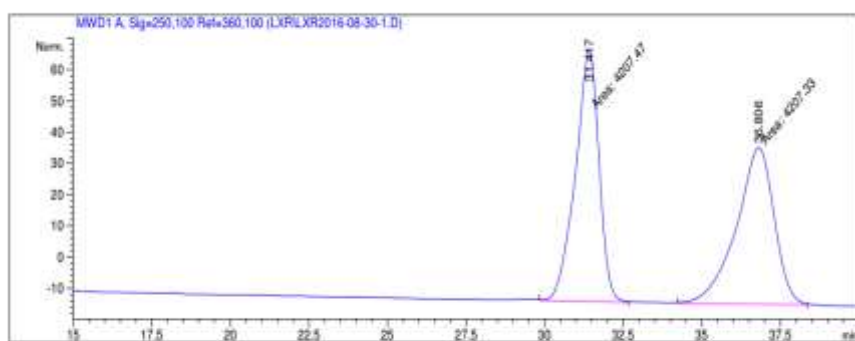


Figure s40. HPLC spectrum for phosphine sulfide **17** in Table 2 Entry 2.

Additional Info : Peak(s) manually integrated



=====
Area Percent Report
=====

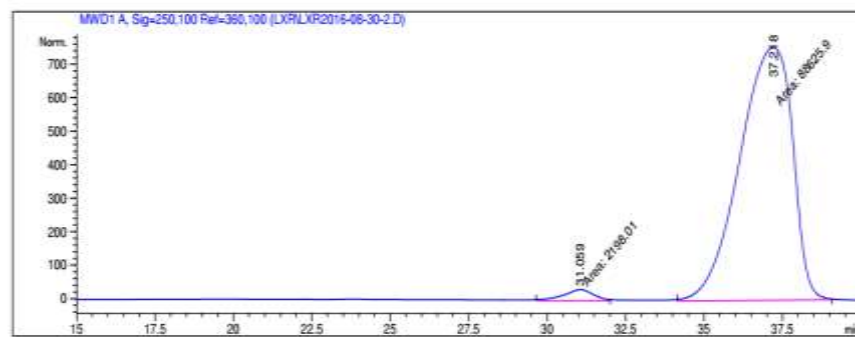
Sorted By : Signal
Multiplier: : 1.0000
Dilution: : 1.0000
Sample Amount: : 1.00000 [ng/uL] (not used in calc.)
Use Multiplier & Dilution Factor with ISTDs

Signal 1: MWD1 A, Sig=250,100 Ref=360,100

Peak #	RetTime [min]	Type	Width [min]	Area [mAU*s]	Height [mAU]	Area %
1	31.417	MM	0.8744	4207.47168	80.20103	50.00008
2	36.806	MM	1.3969	4207.33447	50.19682	49.9992

Figure s41. HPLC spectrum for racemic phosphine sulfide **19**.

Additional Info : Peak(s) manually integrated



=====
Area Percent Report
=====

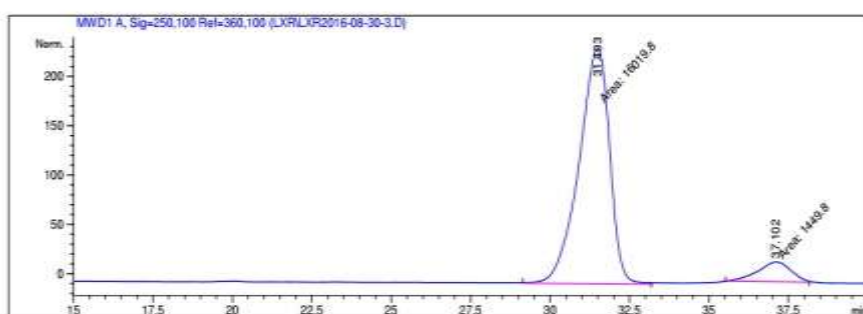
Sorted By : Signal
Multiplier: : 1.0000
Dilution: : 1.0000
Sample Amount: : 1.00000 [ng/uL] (not used in calc.)
Use Multiplier & Dilution Factor with ISTDs

Signal 1: MWD1 A, Sig=250,100 Ref=360,100

Peak #	RetTime [min]	Type	Width [min]	Area [mAU*s]	Height [mAU]	Area %
1	31.059	MM	1.1157	2198.01489	32.83495	2.4201
2	37.218	MM	1.9567	8.86259e4	754.87421	97.5799

Figure s42. HPLC spectrum for phosphine sulfide **19** in Table 2 Entry 3.

Additional Info : Peak(s) manually integrated



=====
Area Percent Report
=====

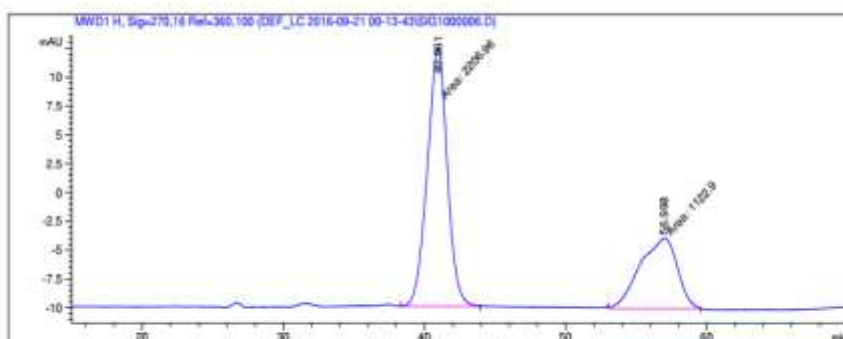
Sorted By : Signal
Multiplier: : 1.0000
Dilution: : 1.0000
Sample Amount: : 1.00000 [ng/ μ l] (not used in calc.)
Use Multiplier & Dilution Factor with ISTDs

Signal 1: MWD1 A, Sig=250,100 Ref=360,100

Peak #	RetTime [min]	Type	Width [min]	Area [mAU*s]	Height [mAU]	Area %
1	31.493	MM	1.1215	1.60198e4	238.07861	91.7010
2	37.102	MM	1.2110	1449.79541	19.95266	8.2990

Figure s43. HPLC spectrum for phosphine sulfide **19** in Table 2 Entry 4.

Additional Info : Peak(s) manually integrated



=====
Area Percent Report
=====

Sorted By : Signal
Multiplier: : 1.0000
Dilution: : 1.0000
Use Multiplier & Dilution Factor with ISTDs

Signal 1: MWD1 H, Sig=270,16 Ref=360,100

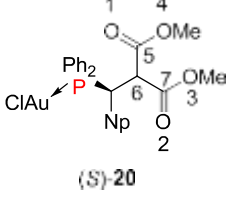
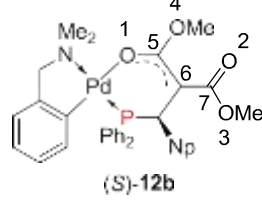
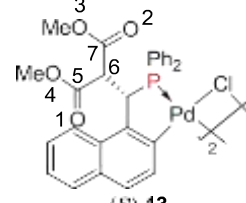
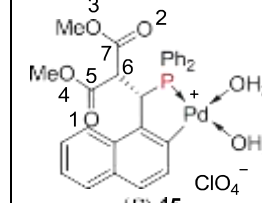
Peak #	RetTime [min]	Type	Width [min]	Area [mAU*s]	Height [mAU]	Area %
1	40.961	MM	1.6429	2206.95605	22.38844	66.2779
2	56.998	MM	1.0691	1122.89709	6.09792	33.7221

Figure s44. HPLC spectrum for phosphine sulfide **17** in Table 2 Entry 5.

Selected Bond Lengths (Å) of Complexes 12b, 13, 15 and 20

The bond lengths of the CO₂Me-moieties in complexes **12b**, **13**, **15** and **20** were collated in Table s1 below. The highlighted bond lengths of complex **12b** indicate the presence of delocalization along the O(1)-C(5)-C(6) moiety.

Table s1. Selected bond lengths (Å) of complexes **12b**, **13**, **15** and **18**.

				
C5-O1	1.182(13)	1.274(5)	1.206(9), 1.202(9)	1.205(7)
C5-O4	1.352(13)	1.355(5)	1.348(8), 1.334(9)	1.336(7)
C5-C6	1.507(17)	1.397(6)	1.527(9), 1.523(9)	1.523(7)
C6-C7	1.531(16)	1.444(6)	1.527(9), 1.528(13)	1.532(17)
C7-O2	1.209(15)	1.216(5)	1.209(9), 1.206(15)	1.205(17)
C7-O3	1.316(15)	1.367(5)	1.332(9), 1.348(17)	1.340(16)

Crystallographic Data

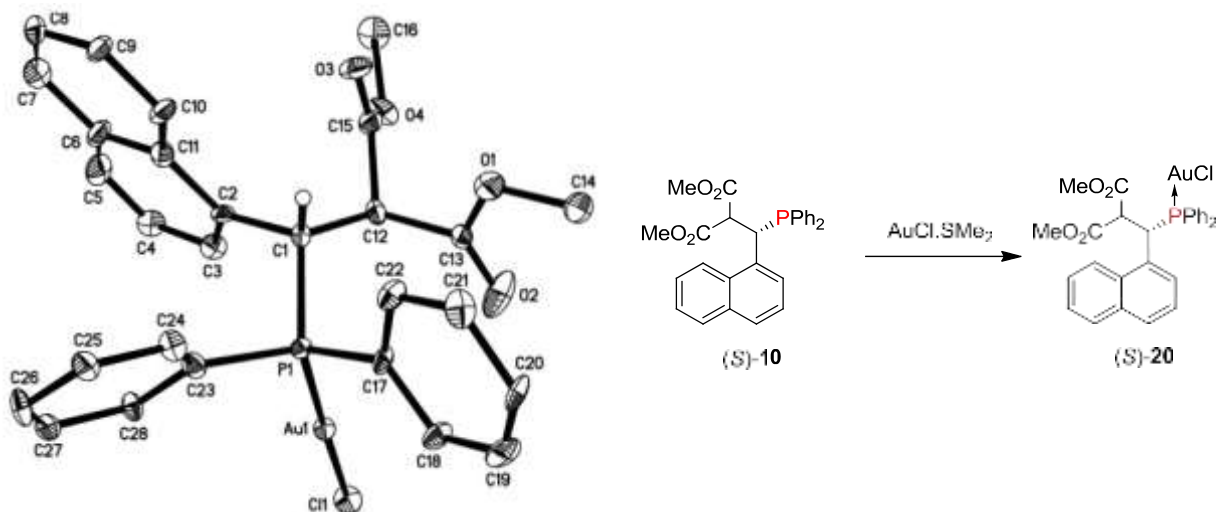


Figure s45. ORTEP structure of chiral phosphine-gold(I) complex (S)-20.

The tertiary phosphine **10** was coordinated onto AuCl to form complex **20**. Recrystallization of the complex from a mixture of DCM/n-hexane afforded single crystals that are suitable for X-ray crystallography. The absolute configuration of the major enantiomer was determined to be *S*.

Table s2. Data collection and structure refinement for complex (S)-20.

Chemical formula	C ₂₈ H ₂₅ AuClO ₄ P	
Formula weight	688.87 g/mol	
Temperature	103(2) K	
Wavelength	0.71073 Å	
Crystal size	0.120 x 0.320 x 0.410 mm	
Crystal habit	colorless block	
Crystal system	monoclinic	
Space group	P 1 21 1	
Unit cell dimensions	a = 9.1660(5) Å	α = 90°
	b = 16.3269(8) Å	β = 115.576(3)°
	c = 9.5017(5) Å	γ = 90°
Volume	1282.62(12) Å ³	
Z	2	
Density (calculated)	1.784 g/cm ³	
Absorption coefficient	5.934 mm ⁻¹	
F(000)	672	
Theta range for data collection	2.38 to 31.16°	
Index ranges	-13<=h<=13, -23<=k<=23, -13<=l<=13	

Reflections collected	21010
Independent reflections	7935 [R(int) = 0.1079]
Coverage of independent reflections	99.8%
Absorption correction	Multi-Scan
Max. and min. transmission	0.5360 and 0.1950
Structure solution technique	direct methods
Structure solution program	XT, VERSION 2014/5
Refinement method	Full-matrix least-squares on F^2
Refinement program	SHELXL-2014/7 (Sheldrick, 2014)
Function minimized	$\Sigma w(F_o - F_c)^2$
Data / restraints / parameters	7935 / 1 / 318
Goodness-of-fit on F^2	0.905
Δ/σ_{\max}	0.001
Final R indices	6509 data; $I > 2\sigma(I)$ R1 = 0.0532, wR2 = 0.1112 all data R1 = 0.0708, wR2 = 0.1219
Weighting scheme	$w=1/[\sigma^2(F_o^2)]$ where $P=(F_o^2+2F_c^2)/3$
Absolute structure parameter	0.016(13)
Largest diff. peak and hole	1.302 and -1.929 eÅ ⁻³
R.M.S. deviation from mean	0.219 eÅ ⁻³

Table s3. Bond lengths (Å) for complex (S)-20.

Au1-P1	2.235(2)	Au1-Cl1	2.283(2)
C1-C2	1.518(14)	C1-C12	1.558(14)
C1-P1	1.847(11)	C2-C3	1.371(14)
C2-C11	1.436(15)	C3-C4	1.420(17)
C4-C5	1.336(18)	C5-C6	1.380(19)
C6-C11	1.428(17)	C6-C7	1.430(18)
C7-C8	1.355(19)	C8-C9	1.390(18)
C9-C10	1.371(16)	C10-C11	1.432(16)
C12-C15	1.507(17)	C12-C13	1.531(16)
C13-O2	1.209(15)	C13-O1	1.316(15)
C14-O1	1.47(2)	C15-O3	1.182(13)
C15-O4	1.352(13)	C16-O4	1.431(15)
C17-C18	1.378(16)	C17-C22	1.395(15)
C17-P1	1.809(11)	C18-C19	1.357(16)
C19-C20	1.346(18)	C20-C21	1.401(18)
C21-C22	1.411(16)	C23-C24	1.381(14)
C23-C28	1.398(15)	C23-P1	1.826(13)
C24-C25	1.367(16)	C25-C26	1.403(19)

C26-C27	1.37(2)	C27-C28	1.406(16)
---------	---------	---------	-----------

Table s4. Bond angles ($^{\circ}$) for complex (S)-**20**.

P1-Au1-C11	178.3(2)	C2-C1-C12	108.8(8)
C2-C1-P1	111.7(7)	C12-C1-P1	113.7(8)
C3-C2-C11	119.4(11)	C3-C2-C1	119.0(10)
C11-C2-C1	121.5(9)	C2-C3-C4	120.9(11)
C5-C4-C3	119.9(11)	C4-C5-C6	121.9(12)
C5-C6-C11	120.2(12)	C5-C6-C7	122.6(12)
C11-C6-C7	117.3(12)	C8-C7-C6	123.0(12)
C7-C8-C9	119.4(12)	C10-C9-C8	121.0(12)
C9-C10-C11	121.1(12)	C6-C11-C10	118.2(11)
C6-C11-C2	117.7(10)	C10-C11-C2	124.1(11)
C15-C12-C13	111.8(9)	C15-C12-C1	106.9(9)
C13-C12-C1	113.8(9)	O2-C13-O1	125.6(12)
O2-C13-C12	122.1(11)	O1-C13-C12	112.3(10)
O3-C15-O4	124.7(11)	O3-C15-C12	125.4(11)
O4-C15-C12	109.9(9)	C18-C17-C22	118.9(10)
C18-C17-P1	120.4(8)	C22-C17-P1	120.6(9)
C19-C18-C17	121.1(11)	C20-C19-C18	121.9(12)
C19-C20-C21	119.3(11)	C20-C21-C22	119.5(10)
C17-C22-C21	119.3(11)	C24-C23-C28	119.0(10)
C24-C23-P1	122.3(8)	C28-C23-P1	118.4(8)
C25-C24-C23	121.8(10)	C24-C25-C26	119.0(11)
C27-C26-C25	120.8(13)	C26-C27-C28	119.5(11)
C23-C28-C27	119.8(9)	C13-O1-C14	114.6(13)
C15-O4-C16	114.8(9)	C17-P1-C23	105.9(5)
C17-P1-C1	106.1(5)	C23-P1-C1	104.2(5)
C17-P1-Au1	113.5(4)	C23-P1-Au1	113.9(4)
C1-P1-Au1	112.4(3)		

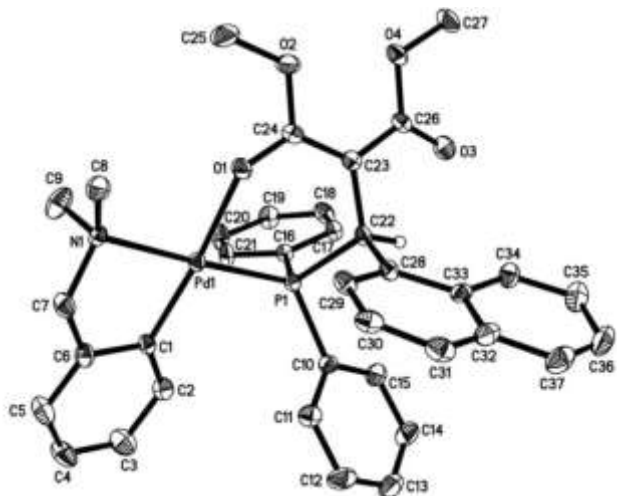


Figure s46. ORTEP structure of chiral phosphine-palladium complex (*S*)-12b.

Table s5. Data collection and structure refinement for complex (*S*)-12b.

Chemical formula	$C_{38}H_{37}Cl_3NO_4PPd$		
Formula weight	815.40 g/mol		
Temperature	153(2) K		
Wavelength	0.71073 Å		
Crystal size	0.380 x 0.400 x 0.420 mm		
Crystal habit	colorless block		
Crystal system	monoclinic		
Space group	P 1 21 1		
Unit cell dimensions	$a = 9.4544(4)$ Å	$\alpha = 90^\circ$	
	$b = 15.4951(6)$ Å	$\beta = 109.9464(16)^\circ$	
	$c = 12.6849(5)$ Å	$\gamma = 90^\circ$	
Volume	$1746.82(12)$ Å ³		
Z	2		
Density (calculated)	1.550 g/cm ³		
Absorption coefficient	0.849 mm ⁻¹		
F(000)	832		
Theta range for data collection	1.71 to 34.03°		
Index ranges	-12≤h≤14, -24≤k≤24, -19≤l≤19		
Reflections collected	38476		
Independent reflections	14147 [R(int) = 0.0777]		
Coverage of independent reflections	99.3%		
Absorption correction	Multi-Scan		
Max. and min. transmission	0.7390 and 0.7170		

Structure solution technique	direct methods
Structure solution program	XT, VERSION 2014/5
Refinement method	Full-matrix least-squares on F^2
Refinement program	SHELXL-2014/7 (Sheldrick, 2014)
Function minimized	$\sum w(F_o - F_c)^2$
Data / restraints / parameters	14147 / 1 / 437
Goodness-of-fit on F^2	1.024
Δ/σ_{\max}	0.001
Final R indices	11864 data; $I > 2\sigma(I)$ $R_1 = 0.0493$, $wR_2 = 0.1081$ all data $R_1 = 0.0656$, $wR_2 = 0.1181$ $w = 1/[\sigma^2(F_o) + (0.0424P)^2 + 0.0709P]$ where $P = (F_o^2 + 2F_c^2)/3$
Absolute structure parameter	-0.017(17)
Largest diff. peak and hole	0.870 and -1.541 e \AA^{-3}
R.M.S. deviation from mean	0.117 e \AA^{-3}

Table s6. Bond lengths (\AA) for complex (S)-12b.

C1-C2	1.400(6)	C1-C6	1.413(6)
C1-Pd1	1.997(4)	C2-C3	1.395(7)
C3-C4	1.367(8)	C4-C5	1.386(7)
C5-C6	1.385(7)	C6-C7	1.503(6)
C7-N1	1.480(6)	C8-N1	1.471(6)
C9-N1	1.487(6)	C10-C11	1.384(7)
C10-C15	1.390(6)	C10-P1	1.823(4)
C11-C12	1.391(7)	C12-C13	1.376(8)
C13-C14	1.386(8)	C14-C15	1.392(7)
C16-C21	1.388(7)	C16-C17	1.390(6)
C16-P1	1.827(4)	C17-C18	1.395(6)
C18-C19	1.385(8)	C19-C20	1.384(7)
C20-C21	1.378(7)	C22-C23	1.510(6)
C22-C28	1.520(6)	C22-P1	1.849(4)
C23-C24	1.397(6)	C23-C26	1.444(6)
C24-O1	1.274(5)	C24-O2	1.355(5)
C25-O2	1.430(6)	C26-O3	1.216(5)
C26-O4	1.367(5)	C27-O4	1.432(6)
C28-C29	1.374(6)	C28-C33	1.445(6)
C29-C30	1.413(7)	C30-C31	1.360(7)
C31-C32	1.422(7)	C32-C37	1.410(7)
C32-C33	1.430(7)	C33-C34	1.420(7)
C34-C35	1.374(7)	C35-C36	1.419(8)

C36-C37	1.350(9)	C38-Cl3	1.739(6)
C38-Cl1	1.746(5)	C38-Cl2	1.777(6)
N1-Pd1	2.144(3)	O1-Pd1	2.123(3)
P1-Pd1	2.2277(10)		

Table s7. Bond angles ($^{\circ}$) for complex (S)-**12b**.

C2-C1-C6	117.4(4)	C2-C1-Pd1	130.7(3)
C6-C1-Pd1	111.8(3)	C3-C2-C1	120.9(4)
C4-C3-C2	120.8(5)	C3-C4-C5	119.3(5)
C6-C5-C4	121.1(5)	C5-C6-C1	120.4(4)
C5-C6-C7	121.6(4)	C1-C6-C7	117.9(4)
N1-C7-C6	108.8(4)	C11-C10-C15	119.3(4)
C11-C10-P1	119.3(3)	C15-C10-P1	121.1(4)
C10-C11-C12	120.0(5)	C13-C12-C11	120.7(5)
C12-C13-C14	119.8(5)	C13-C14-C15	119.8(5)
C10-C15-C14	120.5(5)	C21-C16-C17	119.1(4)
C21-C16-P1	117.9(3)	C17-C16-P1	123.0(3)
C16-C17-C18	120.0(4)	C19-C18-C17	120.1(4)
C20-C19-C18	119.7(4)	C21-C20-C19	120.2(4)
C20-C21-C16	120.8(4)	C23-C22-C28	116.0(3)
C23-C22-P1	113.6(3)	C28-C22-P1	109.8(3)
C24-C23-C26	126.1(4)	C24-C23-C22	119.5(4)
C26-C23-C22	114.3(4)	O1-C24-O2	116.1(4)
O1-C24-C23	126.4(4)	O2-C24-C23	117.5(4)
O3-C26-O4	120.3(4)	O3-C26-C23	124.0(4)
O4-C26-C23	115.7(4)	C29-C28-C33	118.5(4)
C29-C28-C22	121.8(4)	C33-C28-C22	119.7(4)
C28-C29-C30	121.9(4)	C31-C30-C29	121.1(5)
C30-C31-C32	119.5(4)	C37-C32-C31	120.4(5)
C37-C32-C33	119.4(5)	C31-C32-C33	120.1(4)
C34-C33-C32	117.4(4)	C34-C33-C28	123.8(4)
C32-C33-C28	118.7(4)	C35-C34-C33	121.7(5)
C34-C35-C36	119.5(5)	C37-C36-C35	120.4(5)
C36-C37-C32	121.4(5)	Cl3-C38-Cl1	111.8(3)
Cl3-C38-Cl2	110.1(3)	Cl1-C38-Cl2	109.9(3)
C8-N1-C7	109.4(4)	C8-N1-C9	109.6(4)
C7-N1-C9	109.9(4)	C8-N1-Pd1	115.4(3)
C7-N1-Pd1	105.2(2)	C9-N1-Pd1	107.3(3)
C24-O1-Pd1	133.6(3)	C24-O2-C25	116.7(4)
C26-O4-C27	114.7(4)	C10-P1-C16	106.2(2)

C10-P1-C22	100.42(19)	C16-P1-C22	106.36(19)
C10-P1-Pd1	122.52(15)	C16-P1-Pd1	109.67(14)
C22-P1-Pd1	110.42(14)	C1-Pd1-O1	173.37(15)
C1-Pd1-N1	82.32(15)	O1-Pd1-N1	91.12(13)
C1-Pd1-P1	98.78(12)	O1-Pd1-P1	87.82(9)
N1-Pd1-P1	176.45(10)		

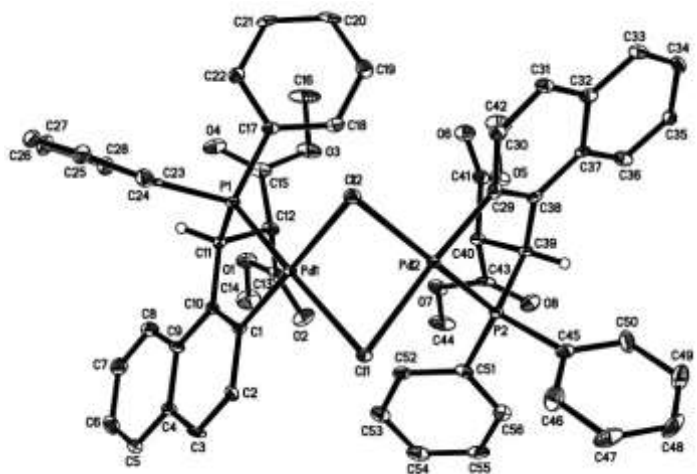


Figure s47. ORTEP structure of chiral phosphine-palladium complex (S)-13.

Table s8. Data collection and structure refinement for complex (S)-13.

Chemical formula	$C_{57}H_{50}Cl_4O_8P_2Pd_2$	
Formula weight	1279.51 g/mol	
Temperature	103(2) K	
Wavelength	1.54178 Å	
Crystal size	0.060 x 0.140 x 0.160 mm	
Crystal habit	yellow block	
Crystal system	monoclinic	
Space group	P 1 21 1	
Unit cell dimensions	$a = 10.97000(10)$ Å	$\alpha = 90^\circ$
	$b = 19.8122(2)$ Å	$\beta = 108.4988(6)^\circ$
	$c = 12.56070(10)$ Å	$\gamma = 90^\circ$
Volume	$2588.89(4)$ Å ³	
Z	2	
Density (calculated)	1.641 g/cm ³	
Absorption coefficient	8.553 mm ⁻¹	
F(000)	1292	
Theta range for data collection	3.71 to 67.52°	
Index ranges	-12≤h≤13, -23≤k≤23, -14≤l≤14	
Reflections collected	29310	
Independent reflections	8900 [R(int) = 0.0486]	
Coverage of independent reflections	97.8%	
Absorption correction	Multi-Scan	
Max. and min. transmission	0.6280 and 0.3420	
Structure solution technique	direct methods	
Structure solution program	XT, VERSION 2014/5	

Refinement method	Full-matrix least-squares on F^2
Refinement program	SHELXL-2014/7 (Sheldrick, 2014)
Function minimized	$\Sigma w(F_o^2 - F_c^2)^2$
Data / restraints / parameters	8900 / 200 / 701
Goodness-of-fit on F^2	1.063
Final R indices	8525 data; $I > 2\sigma(I)$ $R_1 = 0.0325$, $wR_2 = 0.0816$ all data $R_1 = 0.0340$, $wR_2 = 0.0829$ $w = 1/[\sigma^2(F_o^2) + (0.0422P)^2]$ where $P = (F_o^2 + 2F_c^2)/3$
Absolute structure parameter	0.013(8)
Largest diff. peak and hole	0.587 and -1.454 e \AA^{-3}
R.M.S. deviation from mean	0.142 e \AA^{-3}

Table s9. Bond lengths (\AA) for complex (S)-13.

C1-C10	1.380(9)	C1-C2	1.427(9)
C1-Pd1	2.001(6)	C2-C3	1.370(10)
C3-C4	1.424(11)	C4-C5	1.409(10)
C4-C9	1.433(9)	C5-C6	1.362(11)
C6-C7	1.408(11)	C7-C8	1.374(11)
C8-C9	1.411(10)	C9-C10	1.430(9)
C10-C11	1.518(8)	C11-C12	1.555(10)
C11-P1	1.855(6)	C12-C13	1.527(9)
C12-C15	1.527(9)	C13-O2	1.206(9)
C13-O1	1.348(8)	C14-O1	1.452(9)
C15-O4	1.209(9)	C15-O3	1.332(9)
C16-O3	1.468(9)	C17-C18	1.393(10)
C17-C22	1.396(10)	C17-P1	1.822(6)
C18-C19	1.409(10)	C19-C20	1.377(11)
C20-C21	1.381(11)	C21-C22	1.394(10)
C23-C28	1.391(10)	C23-C24	1.396(10)
C23-P1	1.816(7)	C24-C25	1.393(11)
C25-C26	1.382(11)	C26-C27	1.388(11)
C27-C28	1.402(11)	C29-C38	1.387(10)
C29-C30	1.421(9)	C29-Pd2	2.017(7)
C30-C31	1.378(10)	C31-C32	1.416(10)
C32-C33	1.413(10)	C32-C37	1.429(10)
C33-C34	1.376(10)	C34-C35	1.410(10)
C35-C36	1.380(10)	C36-C37	1.413(10)
C37-C38	1.436(10)	C38-C39	1.506(9)
C39-C40	1.564(9)	C39-P2	1.851(6)

C40-C41A	1.52(2)	C40-C43	1.523(9)
C40-C41	1.528(13)	C41-O6	1.206(15)
C41-O5	1.348(17)	C42-O5	1.470(14)
C41A-O6A	1.20(2)	C41A-O5A	1.33(2)
C42A-O5A	1.47(2)	C43-O8	1.202(9)
C43-O7	1.334(9)	C44-O7	1.444(9)
C45-C46	1.388(11)	C45-C50	1.390(10)
C45-P2	1.804(7)	C46-C47	1.403(11)
C47-C48	1.389(13)	C48-C49	1.392(12)
C49-C50	1.381(11)	C51-C52	1.408(10)
C51-C56	1.421(10)	C51-P2	1.797(7)
C52-C53	1.379(10)	C53-C54	1.404(11)
C54-C55	1.398(11)	C55-C56	1.375(11)
C57-Cl4	1.755(10)	C57-Cl3	1.763(8)
Cl1-Pd1	2.4300(15)	Cl1-Pd2	2.4322(15)
Cl2-Pd2	2.4461(17)	Cl2-Pd1	2.4521(14)
P1-Pd1	2.1983(16)	P2-Pd2	2.2008(17)
Pd1-Pd2	2.9813(6)		

Table s10. Bond angles ($^{\circ}$) for complex (S)-13.

C10-C1-C2	119.4(6)	C10-C1-Pd1	123.2(4)
C2-C1-Pd1	117.3(5)	C3-C2-C1	120.9(6)
C2-C3-C4	120.9(6)	C5-C4-C3	121.3(6)
C5-C4-C9	119.8(6)	C3-C4-C9	118.9(6)
C6-C5-C4	121.6(7)	C5-C6-C7	119.3(7)
C8-C7-C6	120.5(7)	C7-C8-C9	121.9(6)
C8-C9-C10	124.4(6)	C8-C9-C4	116.9(6)
C10-C9-C4	118.7(6)	C1-C10-C9	121.2(5)
C1-C10-C11	117.9(5)	C9-C10-C11	120.7(5)
C10-C11-C12	116.6(6)	C10-C11-P1	102.2(4)
C12-C11-P1	109.6(4)	C13-C12-C15	110.7(5)
C13-C12-C11	111.8(5)	C15-C12-C11	109.7(5)
O2-C13-O1	124.2(6)	O2-C13-C12	124.4(6)
O1-C13-C12	111.4(6)	O4-C15-O3	125.1(6)
O4-C15-C12	124.9(6)	O3-C15-C12	110.0(6)
C18-C17-C22	119.5(6)	C18-C17-P1	118.6(5)
C22-C17-P1	121.8(5)	C17-C18-C19	119.8(6)
C20-C19-C18	119.9(7)	C19-C20-C21	120.5(6)
C20-C21-C22	120.2(6)	C21-C22-C17	120.0(6)
C28-C23-C24	120.2(6)	C28-C23-P1	122.1(6)

C24-C23-P1	117.6(5)	C25-C24-C23	120.0(7)
C26-C25-C24	119.6(7)	C25-C26-C27	121.1(7)
C26-C27-C28	119.5(7)	C23-C28-C27	119.6(7)
C38-C29-C30	120.0(6)	C38-C29-Pd2	122.2(5)
C30-C29-Pd2	117.7(5)	C31-C30-C29	120.2(6)
C30-C31-C32	121.3(6)	C33-C32-C31	121.3(6)
C33-C32-C37	119.6(6)	C31-C32-C37	119.0(6)
C34-C33-C32	120.5(6)	C33-C34-C35	120.4(6)
C36-C35-C34	120.1(6)	C35-C36-C37	121.0(6)
C36-C37-C32	118.3(6)	C36-C37-C38	122.8(6)
C32-C37-C38	118.8(6)	C29-C38-C37	120.4(6)
C29-C38-C39	118.2(6)	C37-C38-C39	121.4(6)
C38-C39-C40	113.4(5)	C38-C39-P2	101.7(4)
C40-C39-P2	109.1(4)	C41A-C40-C43	108.(2)
C43-C40-C41	109.9(10)	C41A-C40-C39	115.(4)
C43-C40-C39	110.3(5)	C41-C40-C39	112.0(17)
O6-C41-O5	123.3(15)	O6-C41-C40	125.4(16)
O5-C41-C40	111.1(14)	C41-O5-C42	113.4(14)
O6A-C41A-O5A	129.(3)	O6A-C41A-C40	120.(3)
O5A-C41A-C40	111.(2)	C41A-O5A-C42A	115.(3)
O8-C43-O7	125.0(6)	O8-C43-C40	124.8(6)
O7-C43-C40	110.1(6)	C46-C45-C50	119.4(7)
C46-C45-P2	116.7(5)	C50-C45-P2	123.7(6)
C45-C46-C47	120.1(7)	C48-C47-C46	119.8(7)
C47-C48-C49	119.7(7)	C50-C49-C48	120.3(8)
C49-C50-C45	120.6(7)	C52-C51-C56	118.5(6)
C52-C51-P2	120.9(5)	C56-C51-P2	120.6(5)
C53-C52-C51	120.6(7)	C52-C53-C54	120.2(7)
C55-C54-C53	119.9(7)	C56-C55-C54	120.1(7)
C55-C56-C51	120.7(7)	Cl4-C57-Cl3	111.7(5)
Pd1-Cl1-Pd2	75.64(4)	Pd2-Cl2-Pd1	74.98(4)
C13-O1-C14	115.1(6)	C15-O3-C16	115.0(7)
C43-O7-C44	114.6(6)	C23-P1-C17	105.5(3)
C23-P1-C11	106.7(3)	C17-P1-C11	109.8(3)
C23-P1-Pd1	115.2(2)	C17-P1-Pd1	115.1(2)
C11-P1-Pd1	104.1(2)	C51-P2-C45	103.8(3)
C51-P2-C39	108.8(3)	C45-P2-C39	107.5(3)
C51-P2-Pd2	118.8(2)	C45-P2-Pd2	113.3(2)
C39-P2-Pd2	104.2(2)	C1-Pd1-P1	79.93(18)
C1-Pd1-Cl1	95.85(18)	P1-Pd1-Cl1	170.35(6)
C1-Pd1-Cl2	177.2(2)	P1-Pd1-Cl2	100.86(5)

Cl1-Pd1-Cl2	83.78(5)	C1-Pd1-Pd2	129.3(2)
P1-Pd1-Pd2	124.43(4)	C11-Pd1-Pd2	52.21(4)
Cl2-Pd1-Pd2	52.42(4)	C29-Pd2-P2	80.3(2)
C29-Pd2-Cl1	175.41(19)	P2-Pd2-Cl1	97.72(6)
C29-Pd2-Cl2	98.5(2)	P2-Pd2-Cl2	174.15(6)
Cl1-Pd2-Cl2	83.86(5)	C29-Pd2-Pd1	132.32(19)
P2-Pd2-Pd1	124.32(4)	C11-Pd2-Pd1	52.15(4)
Cl2-Pd2-Pd1	52.60(3)		

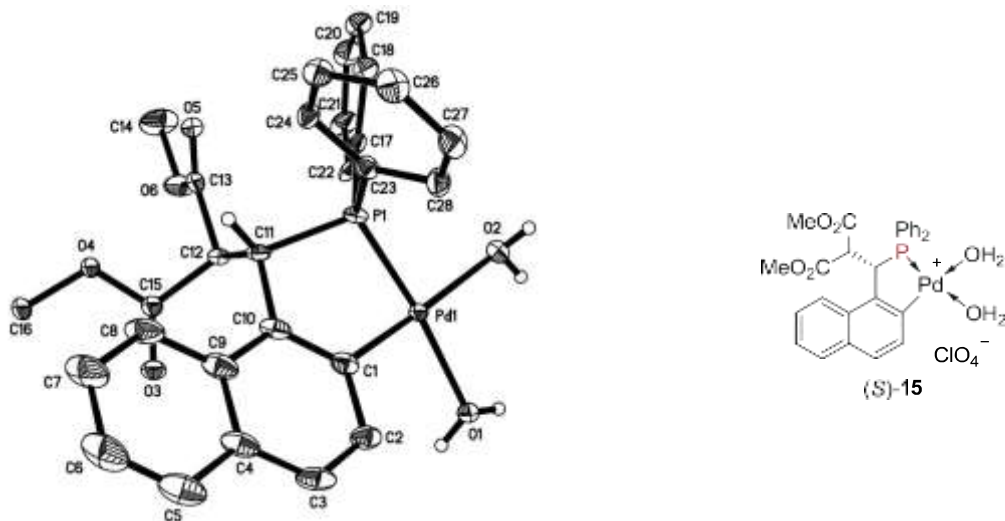


Figure s48. ORTEP structure of chiral phosphine-palladium complex (S)-15.

Table s11. Data collection and structure refinement for complex (S)-13.

Chemical formula	C ₂₈ H ₃₀ ClO ₁₁ PPd	
Formula weight	715.34 g/mol	
Temperature	103(2) K	
Wavelength	1.54178 Å	
Crystal size	0.080 x 0.100 x 0.200 mm	
Crystal habit	colorless block	
Crystal system	orthorhombic	
Space group	P 21 21 21	
Unit cell dimensions	a = 10.62424(9) Å	α = 90°
	b = 10.81406(10) Å	β = 90°
	c = 25.3404(2) Å	γ = 90°
Volume	2911.39(4) Å ³	
Z	4	
Density (calculated)	1.632 g/cm ³	
Absorption coefficient	7.035 mm ⁻¹	
F(000)	1456	
Theta range for data collection	3.49 to 67.38°	
Index ranges	-12<=h<=12, -12<=k<=11, -29<=l<=30	
Reflections collected	14284	
Independent reflections	5015 [R(int) = 0.0321]	
Coverage of independent reflections	99.0%	
Absorption correction	Multi-Scan	
Max. and min. transmission	0.6030 and 0.3340	
Structure solution technique	direct methods	
Structure solution program	XT, VERSION 2014/5	

Refinement method	Full-matrix least-squares on F^2
Refinement program	SHELXL-2014/7 (Sheldrick, 2014)
Function minimized	$\Sigma w(F_o^2 - F_c^2)^2$
Data / restraints / parameters	5015 / 953 / 562
Goodness-of-fit on F^2	1.023
Δ/σ_{\max}	0.001
Final R indices	4886 data; $I > 2\sigma(I)$ $R_1 = 0.0308$, $wR_2 = 0.0822$
	all data $R_1 = 0.0314$, $wR_2 = 0.0826$
Weighting scheme	$w = 1/[\sigma^2(F^2) + (0.0564P)^2]$ where $P = (F_o^2 + 2F_c^2)/3$
Absolute structure parameter	0.011(4)
Largest diff. peak and hole	0.435 and -1.178 e \AA^{-3}
R.M.S. deviation from mean	0.153 e \AA^{-3}

Table s12. Bond lengths (\AA) for complex (*S*)-15.

Pd1-C1	1.997(6)	Pd1-O1	2.172(4)
Pd1-P1	2.1786(12)	Pd1-O2	2.205(4)
C1-C10	1.385(8)	C1-C2	1.418(7)
C2-C3	1.362(9)	C3-C4	1.422(9)
C4-C9	1.424(9)	C4-C5	1.429(9)
C5-C6	1.382(10)	C6-C7	1.396(11)
C7-C8	1.379(9)	C8-C9	1.424(9)
C9-C10	1.438(8)	C10-C11	1.504(8)
C11-C12	1.543(7)	C11-P1	1.857(6)
C12-C13	1.523(7)	C12-C15A	1.528(14)
C12-C15	1.532(17)	C13-O5	1.205(7)
C13-O6	1.336(7)	C14-O6	1.451(7)
C15-O3	1.205(17)	C15-O4	1.340(16)
C16-O4	1.456(15)	C15A-O3A	1.205(14)
C15A-O4A	1.337(13)	C16A-O4A	1.454(14)
C17-C18	1.396(12)	C17-C22	1.421(12)
C17-P1	1.809(9)	C18-C19	1.371(13)
C19-C20	1.401(14)	C20-C21	1.399(14)
C21-C22	1.398(12)	C23-C28	1.396(13)
C23-C24	1.397(13)	C23-P1	1.809(8)
C24-C25	1.385(11)	C25-C26	1.390(14)
C26-C27	1.365(14)	C27-C28	1.397(12)
C17A-C18A	1.39	C17A-C22A	1.39
C17A-P1	1.788(11)	C18A-C19A	1.39
C19A-C20A	1.39	C20A-C21A	1.39

C21A-C22A	1.39	C23A-C24A	1.371(18)
C23A-C28A	1.408(19)	C23A-P1	1.836(12)
C24A-C25A	1.391(19)	C25A-C26A	1.39(2)
C26A-C27A	1.366(18)	C27A-C28A	1.401(16)
Cl1-O9	1.410(10)	Cl1-O7	1.425(10)
Cl1-O8	1.436(8)	Cl1-O10	1.469(9)
Cl1A-O8A	1.410(17)	Cl1A-O9A	1.426(15)
Cl1A-O7A	1.438(17)	Cl1A-O10A	1.455(16)

Table s13. Bond angles ($^{\circ}$) for complex (S)-15.

C1-Pd1-O1	95.30(19)	C1-Pd1-P1	79.32(15)
O1-Pd1-P1	173.80(12)	C1-Pd1-O2	173.14(19)
O1-Pd1-O2	89.05(15)	P1-Pd1-O2	96.60(11)
C10-C1-C2	120.2(5)	C10-C1-Pd1	121.9(4)
C2-C1-Pd1	117.7(4)	C3-C2-C1	120.3(5)
C2-C3-C4	121.3(5)	C3-C4-C9	119.3(5)
C3-C4-C5	121.0(6)	C9-C4-C5	119.8(6)
C6-C5-C4	119.6(7)	C5-C6-C7	121.1(6)
C8-C7-C6	120.2(7)	C7-C8-C9	121.3(7)
C8-C9-C4	118.0(5)	C8-C9-C10	123.6(6)
C4-C9-C10	118.3(6)	C1-C10-C9	120.5(5)
C1-C10-C11	118.3(5)	C9-C10-C11	121.2(5)
C10-C11-C12	116.4(4)	C10-C11-P1	99.9(4)
C12-C11-P1	112.4(3)	C13-C12-C15A	109.8(9)
C13-C12-C15	107.4(11)	C13-C12-C11	110.3(4)
C15A-C12-C11	105.6(11)	C15-C12-C11	116.0(13)
O5-C13-O6	125.1(5)	O5-C13-C12	124.9(5)
O6-C13-C12	110.0(4)	O3-C15-O4	124.(2)
O3-C15-C12	125.(2)	O4-C15-C12	110.3(15)
C15-O4-C16	116.6(12)	O3A-C15A-O4A	124.4(17)
O3A-C15A-C12	124.3(18)	O4A-C15A-C12	111.3(12)
C15A-O4A-C16A	115.9(11)	C18-C17-C22	119.9(8)
C18-C17-P1	125.4(10)	C22-C17-P1	114.7(10)
C19-C18-C17	120.7(10)	C18-C19-C20	119.8(10)
C21-C20-C19	120.6(9)	C22-C21-C20	119.8(9)
C21-C22-C17	118.9(10)	C28-C23-C24	120.0(7)
C28-C23-P1	118.3(7)	C24-C23-P1	121.7(7)
C25-C24-C23	120.2(8)	C24-C25-C26	119.3(8)
C27-C26-C25	121.1(8)	C26-C27-C28	120.5(9)
C23-C28-C27	119.0(8)	C18A-C17A-C22A	120.0

C18A-C17A-P1	117.7(12)	C22A-C17A-P1	122.2(12)
C19A-C18A-C17A	120.0	C18A-C19A-C20A	120.0
C21A-C20A-C19A	120.0	C22A-C21A-C20A	120.0
C21A-C22A-C17A	120.0	C24A-C23A-C28A	120.9(12)
C24A-C23A-P1	119.6(12)	C28A-C23A-P1	119.5(10)
C23A-C24A-C25A	118.9(14)	C26A-C25A-C24A	120.7(15)
C27A-C26A-C25A	120.8(14)	C26A-C27A-C28A	119.6(13)
C27A-C28A-C23A	119.1(12)	C13-O6-C14	115.5(5)
O9-C11-O7	111.5(8)	O9-C11-O8	110.4(7)
O7-C11-O8	108.8(7)	O9-C11-O10	107.9(7)
O7-C11-O10	109.9(7)	O8-C11-O10	108.2(6)
O8A-C11A-O9A	113.4(15)	O8A-C11A-O7A	116.2(16)
O9A-C11A-O7A	105.3(13)	O8A-C11A-O10A	106.9(15)
O9A-C11A-O10A	109.0(12)	O7A-C11A-O10A	105.7(15)
C17-P1-C23	106.8(6)	C17A-P1-C23A	105.9(9)
C17A-P1-C11	112.6(5)	C17-P1-C11	111.8(4)
C23-P1-C11	97.4(4)	C23A-P1-C11	111.9(6)
C17A-P1-Pd1	114.7(6)	C17-P1-Pd1	112.8(4)
C23-P1-Pd1	123.3(3)	C23A-P1-Pd1	108.3(5)
C11-P1-Pd1	103.51(16)		